STIF

NASA CONTRACTOR REPORT 166425

Identification and Stochastic Control of Helicopter Dynamic Modes

J. A. Molusis
Y. Bar-Shalom

GRANT NAG 2-72
January 1983

NASA

NASA CONTRACTOR REPORT 166425

Identification and Stochastic Control of Helicopter Dynamic Modes

J. A. Molusis and Y. Bar-Shalom
University of Connecticut
Storrs, Connecticut

Prepared for
Ames Research Center
under Grant NAG 2-72

National Aeronautics and
Space Administration

Ames Research Center
Moffett Field, California 94035

CONTENTS

SUMMARY

A general treatment of parameter identification and stochastic control for use on helicopter dynamic systems is presented. The emphasis of the work reported herein is on rotor dynamic models, including specific applications to rotor blade flapping and the helicopter ground resonance problem. Dynamic systems which are governed by periodic coefficients as well as constant coefficient models are addressed. The dynamic systems are modeled by linear state variable equations which are used in the identification and stochastic control formulation. The research presented addresses the pure identification problem as well as the stochastic control problem which includes combined identification and control for dynamic systems. The stochastic control problem includes the effect of parameter uncertainty on the solution and the concept of learning and how this is affected by the control's dual effect. The identification formulation requires algorithms suitable for on-line use and thus recursive identification algorithms are considered. The applications presented use the recursive extended Kalman filter for parameter identification which has excellent convergence for systems without process noise. Adaptive control results based upon the certainty equivalence principle are also presented for the rotor blade flap model.

INTRODUCTION

The concept of using active control for helicopter dynamic modes offers the potential for improved helicopter rotor operation. The alleviation of retreating blade stall, improvement in dynamic stability and reduction of vibration through active control are some of the potential improvements to be gained through active control. The current trend toward fly-by-wire computer systems and high frequency rotor control make the concept of active rotor control feasible. Higher harmonic swashplate control and individual blade control permit the use of active control techniques for stochastic control of dynamic modes. Active control of helicopter rotor systems requires the use of parameter identification of dynamic models and either fixed gain or adaptive control laws. The focus of this reasarch is on both pure identification of dynamic models and stochastic control as applied to helicopter dynamic systems.

Until recently most of the research activity in parameter identification has focused on the problem of aerodynamic stability derivative extraction for handling qualities models [1,2,3,4]. The identification of stability and control derivatives for handling quality models is well understood, however by no means completely solved. Rotor blade identification has also been done [5,6] with emphasis on wind tunnel applications. These rotor studies which address the pure identification problem have focused mainly on the physical model requirements and have used off-line type algorithms which do not formally account for random process noise excitation. Thus, applicability to general wind tunnel or flight test useage is limited. An on-line identification procedure was presented in reference 7 for rotor blade mode identification from random wind tunnel turbulence excitation. A recursive maximum likelihood (RML) procedure was used which is unbiased in the presence of both random measurement and process noise. Although the RML procedure was an on-line algorithm and suitable for random turbulence, it is limited to single input-single output systems or autoregressive moving average (ARMA) models.

The general state space identification problem is presented for helicopter rotor dynamic systems. Identification algorithms suitable for both random measurement and process noise are discussed for off-line and on-line use with emphasis on application to helicopter rotor dynamic models.

The studies on control of helicopter systems have primarily focused on handling qualities autopilot design [8] with some research on the gust alleviation problem [9,10,11]. Recently, fully adaptive higher harmonic control (HHC) algorithms which include on-line identification and control have been developed and tested on simulations and in the wind tunnel [12,13,14,15]. These applications are designed to minimize steady helicopter vibration which originate in the rotor. The acceptance and development by the rotorcraft community of high frequency rotor multicyclic hardware have made HHC suitable for flight vehicles. In addition, the present interest in helicopter individual blade control (IBC) [16,17,18] will further open up new areas of application for stochastic control and identification of rotor dynamic systems. Applications to rotor stall alleviation, improved rotor stability and gust alleviation are potential areas of application.

This report presents the general state space formulation for helicopter rotor dynamic systems for parameter identification. The stochastic control formulation is presented which leads to fixed gain feedback controllers as well as adaptive control solutions. The stochastic control approach follows that presented in ref. 19 and 20 which includes the adaptive control properties: (1) caution, (2) probing, and (3) deterministic control.

The theoretical background for identification and stochastic control is presented in Section II. The rotor blade flapping results which include periodic coefficients and reverse flow effects are presented in Section III. Parameter identification resulcs for the helicopter ground resonance model is presented in Section IV.

SYMBOLS

A	Continuous time matrix used for ground resonance model defined in Eq. (3.24)
$A(\Theta(t))$	time-varying matrix as a function of parameters Θ
$a, \bar{a}$	scalar parameter and its mean value, respectively, used in Eq. (2.30)
a_{21}, a_{22}, b_{21}	flapping model periodic coefficients defined in Eq. (3.6) - Eq. (3.8)
$\bar{a}_{21}, \bar{a}_{22}, \bar{b}_{21}$	value of flapping model periodic coefficients at $\mu = 0$
$B(\Theta(t))$	time-varying control matrix as a function of parameters Θ
B	continuous time matrix used for ground resonance model defined in Eq. (3.25)
C	measurement matrix (periodic) used for ground resonance model defined in Eq. (3.26) and Eq. (3.27)
$C(\ )$	N-step cost function defined in Eq. (2.28)
$c[k, \ ]$	cost function evaluated at time step k
$E\{\ \}$	denotes expected value
$E\{\cdot \mid \cdot\}$	denotes conditional expected value
F	discrete transition matrix, approximated as in Eq. (2.6)
$f[\ ]$	general vector nonlinear function
$f_z[\ ]$	partial derivative of f w.r.t. z. (Jacobian matrix)
$f^x[\ ]$	nonlinear function associated with the state equation
$f^\Theta[\ ]$	nonlinear function associated with the parameters, Θ
F_k	value of state transition matrix at time step k, (Eq. 2.58)
$\bar{F}_x$	longitudinal force excitation of support degrees of freedom, $\frac{F_x}{m_x \Omega^2 R}$, R = 20 ft

$\bar{F}_y$	lateral force excitation of support degrees of freedom, $\frac{F_y}{m_y \Omega^2 R}$, R = 20 ft
G	discrete control matrix approximated as in Eq. (2.7)
G_k	value of state transition matrix at time step k, (Eq. 2.58)
H	measurement matrix
H^x	measurement matrix associated with system state vector
h[ ]	general nonlinear measurement function
I^{k+1}	information set at time step k+1, defined in Eq. (2.38)
i	time step number
J	objective function (cost)
$J^*(k,I^k)$	optimal cost-to-go from time k to the end defined in Eq. (2.43)
J_{CAUT}	caution component of the total cost
J_{DET}	deterministic component of the total cost
J_{PROB}	probing component of the total cost
K_k	backward solution of the matrix Riccatti equation computed by Eq. (2.59)
k	time step number
L_k	optimal CE control feedback gain computed by Eq. (2.57b)
L^D	control gain for the deterministic one step example Eq. (2.34)
L^S	stochastic control gain which includes caution given by Eq. (2.35) or Eq. (2.36)
M_β	periodic coefficient associated with β of blade flapping given by Eq. (3.2), $1/sec^2$
$M_{\dot{\beta}}$	periodic coefficient associated with $\dot{\beta}$ of blade flapping given by Eq. (3.3), 1/sec
M_{Θ_R}	periodic coefficient associated with blade angle Θ_R of blade flapping given by Eq. (3.4)
m_x	mass of the longitudinal support degree of freedom, (m_x = 2767 slugs)
m_y	mass of the lateral support degree of freedom (m_y = 2457 slugs)
N	final time step
n_x	number of state variables
n_z	number of state variables plus parameters ($n_z = n_x + n_\Theta$)
n_Θ	number of parameters
P	covariance matrix
p[•|•]	conditional probability density function
Q	cost function weighting matrix on the state
Q^x	process noise covariance on the state equations
Q^Θ	process noise covariance on the parameters

R	cost function weighting matrix on the control (also used as noise covariance on the measurement)
S	innovations covariance defined in Eq. (2.21)
$S(\psi)$	on-off switch to activate reverse flow terms in flapping equation
t	continuous time index, sec
Δt	integration time step, sec
u	control vection
u^D, u^S	deterministic and stochastic control solution defined in Eq. (2.50) through Eq. (2.52)
$v(t)$	continuous time random white process noise
v_k	discrete time random white process noise sequence
v^x, v^Θ	discrete time random white process noise sequence of x and θ eqs
$\bar{v}$	mean value of v
W	Kalman filter gain defined in Eq. (2.24)
w	discrete time random white measurement noise
x	state vector
x^a	augmented state vector ($x^a = \Theta$)
$\hat{x}(k\|k)$	updated state estimate at time k given measurements up to time k
y	measurement vector
z	state vector of states and parameters
$\hat{z}(k\|k)$	updated state estimate (states and parameters) at time k given measurements up to time k
$\tilde{z}$	state error defined in Eq. (2.16)
β	flapping angle of blade, deg
Δ	time step size
γ	Lock number, ($\gamma = 5$)
ζ	blade lag angle, deg
ζ_{1c}	cosing Fourier component of blade lag, deg
ζ_{1s}	sine Fourier component of blade lag, deg.
η_x, η_y	longitudinal and lateral support damping ratio, respectively, % critical
η_ζ	blade inplane damping ratio, % critical
μ	rotor advance ratio, $V/\Omega R$
ν	innovation sequence defined in Eq. (2.20)
Θ	parameter vector
θ_R	rotor blade pitch angle, deg

ρ_{ab}	correlation coefficient
σ	standard deviation
σ_a, σ_b	standard deviation of a and b, respectively
σ_{ab}	square root of the covariance between a and b
Σ	covariance of $\hat{x}$ defined in Eq. (2.48)
ϕ	Jacobian matrix (Eq. (2.19))
$\phi(k,x(k)$	general form of optimal control solution (Eq. (2.51))
ψ	azimuth angle of rotor blade, deg
$\psi[\ ]$	general form of control solution under the separation property (Eq. (2.52))
Ω	angular velocity of rotor, rad/sec (or RPM)
$\bar{\omega}_\zeta$	blade inplane natural frequency ($\div \Omega$)
$\bar{\omega}_x, \bar{\omega}_y$	longitudinal and lateral support natural frequency ($\div \Omega$)
$(\ )^T, (\ )'$	denotes transpose
$(\dot{})$	denotes time derivative

THEORETICAL BACKGROUND

This section presents the basic theoretical background for identification and stochastic control of dynamic systems. A brief description of the identification and stochastic control formulation is presented. This is followed by a more detailed treatment of the identification problem. Finally, the fundamental ideas of stochastic control theory are presented.

Problem Description and Overall Approach

The state variable representation is used to model helicopter rotor rotating coordinates and fixed axis coordinates. Rotating coordinates for either articulated or hingeless rotors include blade flap, lag and torsion, which can also include rotor harmonic inflow coordinates. Fixed axis coordinates include vehicle body motion and landing support degrees of freedom for the ground resonance problem. A discussion of state variable models for articulated and hingeless rotors coupled to fixed axis degrees of freedom is given in ref. 1. The linearized state equations include periodic coefficients and can be represented in either the rotating system or fixed axis system using the multiblade coordinate transformation. The linearized state equations will be used for the parameter identification problem and the stochastic control problem.

The dynamic identification problem is based upon the linear state equations

$$\begin{aligned} x_{i+1} &= F_i(\Theta_i)\, x_i + G_i(\Theta_i)\, u_i + v_i^x \\ \Theta_{i+1} &= \Theta_i \qquad\qquad\qquad\quad + v_i^\Theta \end{aligned} \tag{2.1}$$

where x_{i+1} is a nxl state vector

u_i is a mxl control vector

Θ_i is a pxl vector of unknown parameters to be identified including periodic coefficients

F_i, G_i are matrices as a function of the unknown parameter vector Θ_i

v_i^x, w_i^x are zero mean random white noise guassian sequences

The measurement equation is

$$y_i = H_i(\Theta_i)\, x_i + w_i \tag{2.2}$$

where y_i is a rxl measurement vector

H_i is a rxn matrix of unknown parameters Θ_i

w_i is a zero mean white noise gaussian sequence

The identification objective is to determine estimates of the unknown parameter vector Θ_i and state x_i from the measurements y_i; given control excitation u_i.

The stochastic control objective is to minimize with respect to the control a quadratic function of the state and control

$$J = \min_{u_i} E\left\{\left(\sum_{i=1}^{N-1} x_i^T Q_i x_i + u_i^T R_i u_i\right) + x_N^T Q_N x_N\right\} \qquad (2.3)$$

where $E\{\ \}$ denotes expected value and

Q_i, R_i are weighting matrices on the state and control, respectively

The pure identification problem is concerned with Eq. (2.1) and (2.2). The pure control problem assumes the parameters are known in Eq. (2.1) and (2.2) and the optimal control u_i which minimizes Eq. (2.3) is to be designed. The stochastic control problem [19] simultaneously considers Eq. (2.1) and (2.3) and two such adaptive control designs are shown in block diagram form in Fig. 1. Details of the parameter identification solution and stochastic control solution are presented in the following sections.

Parameter Identification Methods

Parameter identification methods can be categorized as either an off-line or on-line method. Off-line methods usually require a number of passes or iterations over the data set being identified. On-line methods are often recursive and updated estimates are generated based upon past data and current measurements. Table 1 shows off-line and on-line identification methods which are asymptotically unbiased for systems contaminated by process noise, measurement noise, and both process and measurement noise. For systems with only process noise, the least square (LS) method yields identical results for either the off-line or recursive formulation. For systems with measurement noise only, the output error maximum likelihood method is suitable for off-line useage. The

recursive maximum likelihood (RML) method [20] and extended Kalman Filter (EKF) are both suitable for systems with measurement noise contamination. The RML method in [20] is based on single input-single output autoregressive moving average (ARMA) models while the EKF is formulated for state space models. For systems which include both process and measurement noise, the RML method or the "corrected" extended Kalman Filter [21] results in asymptotically unbiased parameter estimates.

Since the state space formulation is used throughout this analysis, the extended Kalman filter is used for parameter identification. Since the EKF results in biased parameter estimates in the presence of process noise, all simulation runs were contaminated with random measurement noise only. A brief description of the convergence characteristics of the EKF used for parameter identification is described below.

The Extended Kalman Filter as an Identification Method and Its Convergence Properties. - The extended Kalman filter (EKF) is a well known method used for estimation of the state and parameters of a dynamic system. The popularity of the EKF as a parameter identification algorithm is due to the fact that the solution is recursive, is relatively simple to implement, and closely resembles the linear Kalman filter solution. It is known that the EKF often fails to converge to the correct parameter values under certain conditions. The first major proof of convergence of the EKF is as presented in Ref. 21 where modifications to the EKF were presented which guarantees convergence to the true parameter values. It was also established that the asymptotic convergence of this modified algorithm is as good as the off-line maximum likelihood (ML) algorithm. Since the off-line ML method is generally accepted as the "standard" for parameter identification, (specially in aircraft applications), this result of Ref. 21 is a significant justification for use of a "modified" extended Kalman filter.

The algorithm being used for this research is the extended Kalman filter (without the modification of Ref. 21), since this algorithm was readily available and was previously implemented in the stochastic control algorithm used in this study. This algorithm provides the state and parameter estimation in the dual control algorithm intended for use in this research. The following summary is presented outlining the convergence properties of this algorithm.

Case 1 - No process noise on the state model (e.g. no wind tunnel turbulence)

a) The EKF yields asymptotically biased estimates of the parameters if the parameter estimate is not close to the true value.

b) The EKF yields asymptotically unbiased estimates of the parameters if the process noise covariance on the parameters is artificially set to a non-zero value.

c) The covariance of the parameter estimate yields an accurate estimate of uncertainty of the parameter estimate for case 1b. This estimate is a close approximation to the Cramer-Rao Error lower bound (ref. 34).

Case 2 - with process noise on the state model

a) The EKF yields asymptotically biased estimates, even when a non-zero value for the parameter process noise covariance is used.

b) The modified EKF of ref. 21 yields asymptotically unbiased estimates of the parameters and convergence is as good as off-line maximum likelihood identification.

The simulations performed in this research are done without process noise and thus the conclusions of case 1 above are applicable. The applications of the EKF algorithm to the flapping model and ground resonance model for the no process noise case is in agreement with the conclusions above for case 1.

The identification application results have been excellent and the details are presented in subsequent sections. The EKF algorithm without the modification of ref. 21 as used in this effort is presented. A brief description of the steps leading to the EKF and resulting equations are given in the next section.

The Extended Kalman Filter Identification Method. - The use of the Extended Kalman Filter for the simultaneous state estimation and parameter identification for a linear system with unknown parameters based on noisy output observations is presented. While this is not an optimal algorithm, its recursive nature and ease of implementation, especially in view of the procedure presented here, make it appealing. Other algorithms, like the Maximum Likelihood (ref 22 and ref. 23) are known to be superior and since they are off-line algorithms are not investigated here.

Consider the linear system described in continuous time by the equation for the n_x dimensional state vector

$$\dot{x}(t) = A(\Theta(t))x(t) + B(\Theta(t))u(t) + v(t) \tag{2.4}$$

where u is the n_u diemsnional control, v the process noise and Θ represents the n_Θ-vector of unknown parameters. The discretized state equation with sampling interval Δ, sufficiently small, i.e., an order of magnitude below the smallest time constant or natural period (inverse of natural frequency). is

$$x(k+1) = F(\Theta(k))x(k) + G(\Theta(k))u(k) + v^x(k) \tag{2.5}$$

where $\Theta(k)$ is the value of the parameter vector during period k,

$$F(\Theta(k)) = I + A(\Theta(k))\Delta \tag{2.6}$$

$$G(\Theta(k)) = B(\Theta(k))\Delta \tag{2.7}$$

and the control u is assumed to have the constant value u (k) during the k-th sampling interval. The discrete-time process noise $v^x(k)$ is assumed to be a zero-mean uncorrelated sequence with known variance matrix Q^x.

Let the measurement equation be

$$y(k) = H^x(k)x(k) + w(k) \tag{2.8}$$

where $H^x(k)$ is the, possibly time-varying, measurement matrix and w(k) the measurement noise. The measurement noise is assumed to be a zero-mean uncorrelated sequence with known covariance matrix R.

The problem is to estimate simultaneously the state x and the parameter vector Θ. If the parameters were known the problem would be a linear one and the Kalman Filter provides the linear minimum mean square error estimate. However, when Θ is not perfectly known a common approach is to use the "Extended Kalman Filter" which estimates the "augmented" state

$$z(k) = \begin{bmatrix} x(k) \\ \Theta(k) \end{bmatrix} \tag{2.9}$$

of dimension

$$n_z = n_x + n_\Theta \tag{2.10}$$

Since elements of the augmented state vector z, namely the components of the proper state x and components of the parameter vector multiply each other in Eq. (2.5) it is obvious that one faces a nonlinear problem. The approach via linearization is described in the next section.

The evolution of the augmented state can be written as

$$z(k+1) = \begin{bmatrix} x(k+1) \\ \Theta(k+1) \end{bmatrix} = \begin{bmatrix} F(\Theta(k)) & 0 \\ 0 & 1 \end{bmatrix} \begin{bmatrix} x(k) \\ \Theta(k) \end{bmatrix} + \begin{bmatrix} G(\Theta(k)) \\ 0 \end{bmatrix} u(k) + \begin{bmatrix} v^x(k) \\ v^\Theta(k) \end{bmatrix} \tag{2.11}$$

where the parameter vector is modelled as a Wiener process driven by the zero-mean uncorrelated noise sequence $v^\Theta(k)$ with an assumed covariance matrix Q^Θ. If the parameters are assumed constant then $Q^\Theta = 0$.

Eq. (2.11) can be written as

$$z(k+1) = f[z(k), u(k)] + v(k) \tag{2.12}$$

and the measurement equation (2.8) becomes, in terms of the augmented state z

$$y(k) = H(k)z(k) + w(k) \tag{2.13}$$

The Extended Kalman Filter equations are obtained as follows. Assume at time k one has the estimate $\hat{z}(k|k)$ and the associated covariance matrix $P(k|k)$. Then the predicted state is obtained by the following first order expansion

$$z(k+1) = f[\hat{z}(k|k),u(k)] + f_z[\hat{z}(k|k),u(k)][z(k) - \hat{z}(k|k)] + v(k) \tag{2.14}$$

where f_z is the Jacobian of the function f with respect to z, evaluated at the latest estimate $\hat{z}(k|k)$. The evaluation of the Jacobian and an automated computer implementation of it are discussed in the Appendix.

The predicted state $\hat{z}(k+1|k)$ is obtained by taking the expected value of (2.14) conditioned on the observations up to and including time k, yielding

$$\hat{z}(k+1|k) = f[\hat{z}(k|k),u(k)] \tag{2.15}$$

where the error

$$\tilde{z}(k|k) \triangleq z(k) - \hat{z}(k|k) \tag{2.16}$$

is assumed zero-mean and thus does not appear in (2.15).

Subtracting (2.15) from (2.14) yields

$$\tilde{z}(k+1|k) \triangleq z(k+1) - \hat{z}(k+1|k) = f_z[\hat{z}(k|k), u(k)][z(k) - \hat{z}(k|k)] + v(k) \tag{2.17}$$

The covariance of the predicted state is thus

$$P(k+1|k) = E[\tilde{z}(k+1|k)\ \tilde{z}'(k+1|k)] = \Phi(k)P(k|k)\Phi'(k) + Q \tag{2.18}$$

where

$$\Phi(k) \triangleq f_z[z(k|k), u(k)] \tag{2.19}$$

The covariance propagation equation (2.18) is the same as for linear systems with the Jacobian taking the place of the transition matrix.

The covariance of the innovation

$$\nu(k+1) \triangleq y(k+1) - H(k+1)\hat{z}(k+1|k) \tag{2.20}$$

is

$$S(k+1) = H(k+1)P(k+1|k)H'(k+1) + R \tag{2.21}$$

as in the linear case.

The state and covariance update are given by the standard equations

$$\hat{z}(k+1|k+1) = \hat{z}(k+1|k) + W(k+1)\nu(k+1) \tag{2.22}$$

$$P(k+1|k+1) = [I - W(k+1)H(k+1)]P(k+1|k) \tag{2.23}$$

where the filter gain is

$$W(k+1) = P(k+1|k)H'(k+1)S^{-1}(k+1) = P(k+1|k+1)H'(k+1)R^{-1} \tag{2.24}$$

The alternate expression for the updated covariance is numerically more stable

$$P(k+1|k+1) = P(k+1|k) - P(k+1|k)H'(k+1)S^{-1}(k+1)H(k+1)P(k+1|k) \tag{2.25}$$

than (2.23).

A similar linearization can be carried out for the measurement equation when it is nonlinear.

Stochastic Control Theory

The problem of stochastic control - control of uncertain systems where the uncertainty is modeled in probabilistic terms - consists, at first sight, of the following subproblems

(i) extraction of information from the system (estimation/identification)

(ii) control of the system based on this information

The topic of this section is the intimate connection between the above two functions, which, in general, cannot be separated.

The next section introduces the assumptions of the Bayesian Stochastic Control framework. The effect of parameter uncertainty on the solution of a simple stochastic control problem, which usually leads to "caution" on the part of the controller, is shown to be not necessarily intuitively predictable. This section also introduces the concept of learning and how this is affected by the control's dual effect. The Principle of Optimality for stochastic systems together with the resulting stochastic dynamic programming equation are presented. As a consequence of the Principle of Optimality for stochastic systems the optimal controller has to anticipate (causally) the future system uncertainties. Specifically, the availability of future observations and the accuracy of future state/parameter estimates enter into the controller's decision about the current control value. This opens the way for actively adaptive controllers that can reduce system uncertainties via the dual effect and then enhance state/parameter estimation to ultimately improve control performance. Finally, the intimate connection between the control's dual effect and Certainty Equivalence property of the optimal stochastic control for a class of systems is given.

The Basic Modeling Assumptions in Stochastic Control - The Bayesian Approach. - In the Bayesian approach for the control of uncertain systems the uncertainties are modeled in probabilistic form. Imperfectly known initial states and system parameters are modeled as random variables while input and output disturbances are modeled as white noise sequences. The distinction between states and parameters is somewhat fuzzy - the latter are varying much slower than the former. In view of this they are sometimes lumped together in what is called augmented state.

The general model of a discrete-time system with unknown (and possibly time-verying) parameters can be written as

$$x(k+1) = f^{x}[k, x(k), \Theta(k), u(k), v^{x}(k)] \tag{2.26a}$$

$$\Theta(k+1) = f^{\Theta}[k, \Theta(k), v^{\Theta}(k)] \tag{2.26b}$$

$$y(k) = h\ [k, x(k), w(k)] \tag{2.26c}$$

where x is the (proper) state vector, Θ the parameter vector, u the control, v^{x} the state process noise, v^{Θ} the parameter process noise, y the measurement (output) and w the measurement noise. With the augmented state $x^{a} = [x'\ \Theta']'$, (2.26) can be written as

$$x^{a}(k+1) = f\ [k, x^{a}(k), u(k), v(k)] \tag{2.27a}$$

$$y(k) = g\ [k, x^{a}(k), w(k)] \tag{2.27b}$$

The reason for the noises being modeled as white is to have x^{a} a Markov process and then (and only then) its pdf (probability density function) $p[x^{a}(k)|Y^{k},U^{k-1}]$ conditioned on the available measurements $Y^{k} = \{y(j),j=0,\ldots,k\}$ and past controls $U^{k-1} = \{u(j),j=0,\ldots,k-1\}$ summarizes the past and constitutes the "information state" for the stochastic problem (see Ref. 24).

The Bayesian approach consists of minimizing the expected value of a cost function (or maximizing a utility function). While other approaches like minimax or worst distribution have been also considered, they are less tractable for closed form solution. Consider, for system (2.26), a fixed end-time problem of N steps with the usual cost

$$C(0, X^{N}, U^{N-1}) = c[N, x(N)] + \sum_{k=0}^{N-1} c[k, x(k), u(k)] \tag{2.28}$$

where $X^{N} = \{x(k), k=0,\ldots,N-1\}$. The stochastic control problem is then

$$\min_{U^{N-1}} E[C] \tag{2.29}$$

In order for the above expectation to exist it is necessary that every variable entering directly or indirectly into (2.28) be either deterministic (i.e., perfectly known) or random with a suitable pdf attached to them. Thus "unknown constant parameters" are modeled as a realization of random variables according to their pdf.

Furthermore the implications of the expectation in (2.29) are that we want to find the optimal control policy over the ensemble of all possible initial states parameters and disturbances. The fact that the optimum is sought for the ensemble of possible parameters (i.e. different realizations of the plant)

is an important point. This has an implication on the control's "adaptation" as will be discussed later.

Parameter Uncertainty and Learning.- Representation (2.26) of a system is more convenient than the augmented system (2.27) when (2.26a) is linear in x, u and v^x, i.e., with known parameters the system would be linear. Consider such a system (scalar for the purpose of this discussion)

$$\begin{aligned} x(k+1) &= a\, x(k) + b\, u(k) + v(k) \\ \Theta(k+1) &= [a\ b]' = \Theta(k) \\ y(0) &= x(0) \end{aligned} \tag{2.30}$$

where v(k) is a zero-mean white noise.

First let N = 1, i.e., a single step problem with cost

$$C = x^2(1) \tag{2.31}$$

The optimal stochastic control for this (static) problem is

$$u^S(0) = -L^S\, x(0) \tag{2.32}$$

where the control gain for the stochastic situation is

$$L^S = \frac{E[a\ b]}{E[b^2]} = \frac{\bar{a}\,\bar{b} + \rho_{ab}\,\sigma_a\,\sigma_b}{\bar{b}^2 + \sigma_b^{\,2}} \tag{2.33}$$

If $\sigma_a = \sigma_b = 0$ the control gain for the corresponding deterministic situation is

$$L^D = \frac{\bar{a}}{\bar{b}} \tag{2.34}$$

The effect of uncertainty can be a <u>decrease</u> or an <u>increase</u> in the control gain:

(i) If $\sigma_a = 0$

$$L^S = \frac{\bar{a}\,\bar{b}}{\bar{b}^2 + \sigma_b^2} < L^D \tag{2.35}$$

i.e., "caution" will be exercised by the controller because of parameter uncertainty.

(ii) If $\bar{a} = \bar{b} = 1$, $\sigma_b^2 = 1$

$$L^S = \frac{1 + \rho_{ab}\,\sigma_a}{2} \; ; \; L^D = 1 \qquad (2.36)$$

and clearly one can have $L^S > L^D$

Thus the effect of the parameter uncertainty has to be analyzed individually for each problem - even in a simple static case the results are not necessarily intuitively predictable.

In multistage control problems for systems with unknown constant parameters the initial parameter uncertainty is modeled by a prior pdf $p[\Theta|I^0]$ where I^0 is the initial information. The initial control u(0) will (among other things) account for the fact that it is applied to a system with parameter $\underline{\Theta}$ "drawn" from the prior pdf. Having assumed the parameter as time-invariant one can expect that the initial uncertainty about the parameter's true value will be reduced in the course of the control process - the controller can "learn" it. Thus, as new information is gathered from measurements, the controller can adapt itself to the particular system it is controlling.

Consider again system (2.30) in the multistage situation with known a and unknown b. Assume the pdf of b to be Gaussian with mean $\hat{b}_0$ and variance σ_0^2 and the variance of v to be σ^2. Due to the linearity of the estimation problem for b, one obtains the recursion for its variance

$$\sigma_{k+1}^{\;2} = \mathrm{var}[b|I^{k+1}] = \sigma^2[u^2(k) + \sigma^2\,\sigma_k^{-2}]^{-1} \qquad (2.37)$$

where

$$I^{k+1} = \{Y^{k+1},\, U^k\} \qquad (2.38)$$

is the information set at k+1.

Thus the prior uncertainty is reduced but it also depends on the control - the control has a <u>dual effect</u> (Ref. 25):

(i) has an effect on the state

(ii) affects subsequent information accuracy - parameter identification in this case.

This suggests that the control could be used to enhance the identification process while controlling the system by "probing" it (Ref. 25) in order to increase the accuracy of subsequent control actions. Such a controller is called dual or <u>actively adaptive</u>.

The Principle of Optimality for Stochastic Systems. - The Principle of Optimality (Ref. 26) for the control of a stochastic system can be stated as follows: at any time, whatever the present information and past decisions, the remaining decisions must constitute an optimal policy with regard to the current information set.

Since the principle of optimality states that every end part of the decision process must be optimal, the multistage optimization has to be started from the last stage. The last decision, u(N-1), must be optimal with regard to the information set available when it has to be computed, i.e., it will be obtained from the functional minimization

$$\min_{u(N-1)} E(C|I^{N-1}) \tag{2.39}$$

where C is the cost for the entire problem.

The next to the last decision, u(N-2)

1) must be optimal with respect to (w.r.t.) I^{N-2} and
2) is to be made knowning that the remaining decision u(N-1) will be optimal w.r.t. $I^{N-1} \supset I^{N-2}$.

Thus, the (functional) minimization that yields the decision function at N-2 is

$$\min_{u(n-2)} E\left[\min_{u(N-1)} E(C|I^{N-1})|I^{N-2}\right] \tag{2.40}$$

and it uses the result of the functional minimization (2.39).

Note that the outside averaging in (2.40) is over y(N-1) using the conditional density

$$p[y(N-1)|I^{N-2}, u(N-2)] \tag{2.41}$$

parameterized by the control at N-2. Since this measurement is not yet available when u(N-2) is to be computed but it will be available for u(N-1) it is "averaged out" in (2.40).

The above-described last two steps are entirely similar to the "preposterior analysis" technique from the operations research literature discussed, e.g., in reference 27. This technique is usually formulated in the following context. The first decision (here u(N-2)] is for information gathering by an experiment from which a posterior information will result [here y(N-1)]

that will be used to make the last decision [here u(N-1)]. The prior (to the experiment) probability density of the (posterior) result of the experiment is called the "preposterior density" and in the present problem this is (2.41). Thus, one can say that preposterior analysis, which is "anticipation" (in a statistical sense, i.e., causal) of future information is a consequence of the principle of optimality.

This "causal anticipation" of future information is the key issue in obtaining a dual controller.

The extension of (2.41) to the full N-stage process yields the optimal expected cost starting from the initial time as

$$J^*(0,I^0) = \min_{u(0)} E\left\{ \dots \min_{u(N-2)} E\left[\min_{u(N-1)} E(C|I^{N-1})|I^{N-2} \dots |I^0 \right] \right\} \qquad (2.42)$$

where I^0 is the initial information. Note that this equation does not assume any particular form for the cost function C.

For the additive cost given by (2.28) one obtains from (2.42), after some manipulations (see, e.g., Ref. 24), the backward recursion known as Bellman's equation or stochastic dynamic programming

$$J^*(k,I^k) = \min_{u(k)} E\{c[k,x(k),u(k)] + J^*(k+1, I^{k+1})|I^k\} \qquad k=N-1,\dots,0 \qquad (2.43)$$

where $J^*(k,I^k)$ is the optimal cost-to-go from time k to the end and its dependence on the available information set at k is explicitly pointed out. The terminal condition for (2.43) is

$$J^*(N,I^N) = E\{c[N,x(N)]|I^N\} \qquad (2.44)$$

where the last measurement is irrelevant since it is averaged out immediately.

The deterministic dynamic programming equation - similar to (2.43) except without the expectation and with I^k replaced by x(k) - can be solved only when an explicit expression of the optimal cost-to-go can be obtained recursively. Otherwise numerical techniques have to be used, but they are of limited usefulness due to the "curse of dimensionality" - the number of required quantization points in the state space increases exponentially with the dimension of the problem.

The stochastic dynamic programming equation (2.43) has the additional problem of averaging over the next measurement [as indicated in (2.41)] and over the state conditioned on the current information set. All this causes the practical usefulness of (2.43) to be of limited value and indicates the need to find suboptimal controllers by suitable approximation of (2.43). The discussion from the last section indicated the two features that a stochastic controller should have

(i) caution

(ii) probing via the dual effect

The approximations of the stochastic dynamic programming fall in the following two classes.

1) *Feedback Type Algorithms:* In this case the control depends only on the current information

$$u(k) = u(k, I^k) \tag{2.45}$$

but does not use the prior statistical description of the future posterior information

$$p[y(j+1)|I^j], \quad j \geq k. \tag{2.46}$$

2) *Closed-Loop Type Algorithms:* Such a controller utilizes feedback (2.45) and anticipates future feedback via (2.46), i.e., that the loop will stay closed.

It is clear that an approximation of (2.43) that has both the features of caution and probing will have to be of the closed-loop type.

The Control's Dual Effect and Certainty Equivalence. - Based on the discussion of the previous sections, the control is said to have a dual effect if the uncertainty about the stochastic system's state (augmented to include the unknown system parameters; superscript a is deleted for simplicity) depends on past control values. This can be formalized as follows. Let

$$\hat{x}(k|k) = E[x(k)|I^k] \tag{2.47}$$

$$\Sigma(k|k) = E\{[x(k) - \hat{x}(k|k)][x(k) - \hat{x}(k|k)]'|I^k\} \tag{2.48}$$

Then, if the covariance (2.48) of the augmented state does not depend on U^{k-1} the control has no dual effect (or second order) - the control is neutral.

Otherwise it has the dual effect since it affects the uncertainty about the augmented state x(k).

It should be pointed out that the dual effect of the control is not limited to systems with unknown parameters but occurs in general in nonlinear systems.

The dual effect of the control and the Certainty Equivalence (CE) property of the optimal stochastic control have been shown to be inter-related for a class of problems (Ref. 28).

The CE property is defined as follows. Consider the stochastic problem (2.29) with an arbitrary cost for system (2.27). Let the corresponding deterministic problem be

$$\min_{U^{N-1}} \; C \tag{2.48}$$

for system

$$\begin{aligned} x(k+1) &= f[k, x(k), u(k), \bar{v}(k)] \\ y(k) &= x(k) \end{aligned} \tag{2.49}$$

where the noise has been replaced by its mean $\bar{v}$. The solution to this deterministic problem in feedback form can be written as

$$u^D(k) = \phi[k, x(k)] \tag{2.50}$$

If the optimal solution to the stochastic problem (2.4), (2.2) is

$$u^S(k) = \phi[k, \hat{x}(k|k)] \tag{2.51}$$

i.e., it is the same as the deterministic one except that the state is replaced by its conditional mean, then the stochastic controller has the CE property. In other words the "control law" ϕ is the same, only the state estimate replaces the state. As will be indicated later the CE property holds under rather restrictive conditions.

If the control law is different, but still uses as input only the state estimate

$$u^S(k) = \psi[k, \hat{x}(k|k)] \tag{2.52}$$

one has the weaker property of separation - there is an estimator cascaded with

a controller. A problem where separation holds but not CE is the so-called Linear-Exponential-Quadratic-Gaussian (LEQG) problem (Ref. 29).

The following result (Ref. 28) connects the control's dual effect to the CE property.

Theorem. For the linear system with additive zero-mean white noise

$$x(k+1) = F(k)\, x(k) + G(k)\, u(k) + v(k) \tag{2.53a}$$

with observation of the general form

$$y(k) = h[k, x(k), w(k)] \tag{2.53b}$$

and quadratic cost

$$C = x'(N)Q(N)x(N) + \sum_{k=0}^{N-1} x'(k)Q(k)x(k) + u'(k)R(k)u(k) \tag{2.54}$$

the optimal stochastic controller that minimizes the expected value of (2.54) has the CE property if and only if the control has no dual effect (of second order). Then

$$u^S(k) = L(k)\, \hat{x}(k|k) \tag{2.55}$$

where $L(k)$ is the same feedback gain as in the corresponding deterministic problem.

Note that, in general, when there are nonlinear observations the estimation accuracy $\Sigma(k|k)$ is control-dependent. In the case of linear observations, however, there is no dual effect and (2.55) holds. This is the reason for the popularity of the LQG problem whose solution is the cascaded linear deterministic feedback with the Kalman filter that yields $\hat{x}(k|k)$.

The CE result has been used in the context of adaptive control as follows. For the system with unknown parameters

$$\begin{aligned} x(k+1) &= F(k,\Theta)\, x(k) + G(k,\Theta)\, u(k) + v(k) \\ y(k) &= H(k)\, x(k) + w(k) \end{aligned} \tag{2.56}$$

with quadratic cost (2.54) one can break down the problem into two parts

(i) estimation/identification

(ii) control (using latest estimates)

The controller can be taken as

$$u(k) = L[k,\hat{\Theta}(k)]\ \hat{x}(k|k) \tag{2.57a}$$

where $\hat{\Theta}(k)$ is the estimate of Θ at time k and it is used in the feedback gain L as if it were the true value. This control, can be called as Heuristic Certainty Equivalence (HCE) because the CE property does not hold in this problem. Note that this controller does not account for the uncertainty in $\hat{\Theta}$ (no caution) nor does it account for the opportunity of probing the system. Nevertheless, controllers of this type, which include the Self-Tuning Regulator have been used very successfully (Ref. 30).

The optimal feedback gain for the HCE controller is

$$L_k = (R_k + G_k' K_{k+1} G_k)^{-1} G_k' K_{k+1} F_k \tag{2.57b}$$

where

$$\begin{aligned} L_k &= L(k, \Theta(k)) \\ F_k &= F(k, \Theta(k)) \\ G_k &= G(k, \Theta(k)) \end{aligned} \tag{2.58}$$

The matrix K_k is given by the backwards iteration solution of the Riccatti equation

$$\begin{aligned} K_k &= F_k' [K_{k+1} - K_{k+1} G_k' (R_k + G_k' K_{k+1} G_k)^{-1} G_k K_{k+1}] F_k + Q_k \\ K_N &= Q_N \end{aligned} \tag{2.59}$$

The optimal feedback gain given by Eq. (2.57) and (2.59) is the same as in the deterministic problem.

The structure of the solution for the optimal control u(k) of Eq. (2.57) is the same as the LQG solution (Ref. 31).

The HCE type controller is of the feedback or passively adaptive type. A closed-loop type "dual" controller, which is actively adaptive, was developed in Tse and Bar-Shalom (Ref. 32, 33, and 19). For further discussion on the quantification of the caution and probing concepts see reference 24.

ROTOR BLADE FLAP IDENTIFICATION AND CONTROL

This section summarizes the results of application of the EKF identification method and the stochastic control solutions as discussed in the previous section. The methods are applied to a single flapping rotor blade modeled by both constant and periodic coefficients.

Rotor Blade Flap Model

The rotor blade flap model used in the simulation analysis includes periodic coefficients and the effects of reverse flow for rotor azimuth ψ greater than 180° and less than 360°. The equations are linear in the state and modeled explicitly as a function of advance ratio in order to investigate the increased effects of periodicity and reverse flow as advance ratio is increased.

The rotor blade flap model equations were taken from ref. 38 and are shown in Eq. (3.1) through Eq. (3.4).

$$\ddot{\beta} + \Omega^2\beta = \gamma[M_{\dot{\beta}}\dot{\beta} + M_{\beta}\beta + M_{\Theta_R}\Theta_R] \tag{3.1}$$

$$M_{\beta} = -\mu\cos\psi(1/6 + 1/4\ \mu\sin\psi - s(\psi)\ \frac{\mu}{6}^3\ \sin^3\psi)\ \Omega^2 \tag{3.2}$$

$$M_{\dot{\beta}} = (-\ 1/8 - 1/6\ \mu\sin\psi - s(\psi)\ \frac{\mu}{12}^4\ \sin^4\psi)\ \Omega \tag{3.3}$$

$$M_{\Theta_R} = (1/8 + 1/3\ \mu\sin\psi + 1/4\ \mu^2\sin^2\psi - s(\psi)\ \frac{\mu}{12}^4\ \sin^4\psi)\ \Omega^2 \tag{3.4}$$

The reverse flow terms are effective for $180^\circ < \psi < 360^\circ$ using the on-off switch

$$s(\psi) = \begin{cases} 0 & , \quad 0 < \psi \leq 180^\circ \\ 1 & , \quad 180^\circ < \psi < 360^\circ \end{cases}$$

The blade flap model was simulated at Ω = 320 RPM with a Lock number γ = 5. Advance ratios of μ = 0 to μ = .8 are investigated.

The discrete state space representation of Eq. (3.1) through Eq. (3.4) is

$$\begin{vmatrix} \bar{x}_1(k+1) \\ \bar{x}_2(k+1) \end{vmatrix} = \begin{vmatrix} \bar{1} & \bar{\ } \\ a_{21} & a_{22} \end{vmatrix} \begin{vmatrix} \bar{x}_1(k) \\ \bar{x}_2(k) \end{vmatrix} + \begin{vmatrix} \bar{0} \\ b_{21} \end{vmatrix} u(k) \tag{3.5}$$

where the discrete coefficients a_{21}, a_{22} and b_{21} are obtained using the first order continuous to discrete approximation of Eq. (2.6) and (2.7).

The A and B matrix elements are

$$a_{21} = \bar{a}_{21} - \theta_1 \cos\psi - \theta_3 \sin\psi \cos\psi + \theta_4 \, s(\psi) \sin^3\psi \cos\psi \qquad (3.6)$$

$$a_{22} = \bar{a}_{22} - \theta_2 \sin\psi - \theta_5 \, s(\psi) \sin^4\psi \qquad (3.7)$$

$$b_{21} = \bar{b}_{21} + \theta_6 \sin\psi + \theta_7 \sin^2\psi - s(\psi) \, \theta_8 \sin^4\psi \qquad (3.8)$$

where the reverse flow switch $s(\psi)$ is defined as before.

The parameter vector for identification is

$$\theta^T = [\bar{a}_{21} \;\; \bar{a}_{22} \;\; \bar{b}_{21} \;\; \theta_1 \;\; \theta_2 \;\; \theta_3 \;\; \theta_4 \;\; \theta_5 \;\; \theta_6 \;\; \theta_7 \;\; \theta_8] \qquad (3.9)$$

where parameters θ_1 through θ_8 are coefficients of periodic terms.

In order to assess the importance of the individual periodic terms the magnitude of the parameter vector θ is tabulated in Table 2 for increasing advance ratio from $0 \leq \mu \leq .8$. For $\mu = 0$ there is no periodicity, $\mu = .2$ shows weak periodicity and negligible reverse flow, $\mu = .5$ shows strong periodicity and some reverse flow, and $\mu = .8$ shows strong periodicity and reverse flow.

The next section summarizes the results obtained for pure identification over an advance ratio range of $\mu = 0$ to $\mu = .8$. Stochastic control applications are then presented.

Parameter Identification Results

The parameter identification formulation was discussed in section II which presented the state variable description (Eq. (2.1) and Eq. (2.2)) for use with the EKF. The state variable flapping model used in the identification is given by Eq. (3.5) with coefficients defined in Eq. (3.6) to Eq. (3.8).

All pure identification results assume a pulse input excitation θ_R for a duration of one sample period ($\Delta t = .005$). The magnitude of the input is such as to yield an initial condition on $\dot{\beta} = 35 \frac{\text{deg}}{\text{sec}}$ for adequate system excitation. This corresponds to an input amplitude of $\theta_R = 10$ deg. The time history response for β and $\dot{\beta}$ is shown in figure 2. The single blade measurement β is used in all runs. The damping ratio is $\zeta = .316$ $(\gamma/16)$ and for $\Omega = 33.51$ rad/sec (320 RPM), the damping factor $\zeta\omega_n$ is 10.47. The flapping time constant is .0955 seconds.

Identification results at hover, $\mu = 0$. - Since there is no periodicity for $\mu = 0$, only two parameters are identified from the initial condition response of figure 2. The parameter vector is

$$\Theta^T = [\bar{a}_{21} \quad \bar{a}_{22}] \tag{3.10}$$

Two noise levels were used in the simulation, a high noise case $2\sigma_v = .08$ deg and a low noise case $2\sigma_v = .008$ deg. The high noise case is approximately a 20% noise-to-signal ratio and the low noise case is approximately 2% noise on the flapping signal β.

Identified parameter convergence is shown in figure 3 for the high noise case (20% noise) and in figure 4 for the low noise case (2% noise). In both cases convergence to the simulation value occurs in less than 1/2 of a rotor revolution. Parameter convergence occurs in a 1/4 of a revolution for the low noise case. Initial starting values for the parameters $\hat{a}_{21}$ and $\hat{a}_{22}$ and standard deviations are also shown. The standard deviations are computed from the Cramer-Rao lower bound, which for no process noise is accurately represented by the covariance equation of the Kalman Filter (ref. 34).

Identification results at $\mu = .2$. - The flapping model of Eq. (3.6) through Eq. (3.8) shows analytic expressions for the state variable A-matrix elements a_{21} and a_{22}. These elements are plotted in fig. 5 for advance ratio $\mu = .2$. Small periodicity is shown vs rotor revolution which also show negligible reverse flow effects. Since, the reverse flow effects are negligible for this case, only the parameter associated with $\sin\psi \cos\psi$ is identified. The parameter vector for identification is

$$\Theta^T = [\Theta_1 \quad \Theta_2 \quad \Theta_3] \tag{3.11}$$

The constant terms $\bar{a}_{21}$ and $\bar{a}_{22}$ in Eq. (3.9) are assumed known, being identified previously at $\mu = 0$ otherwise a longer data record would be required.

Figure 6 shows the identified parameter convergence for $\mu = .2$ and low noise for the periodic coefficients Θ_1, Θ_2 and Θ_3. Excellent identification is shown with convergence occurring less than 1 rotor revolution. The computed standard deviation bands are also shown in fig. 6 which indicate excellent accuracy.

Identification results at $\mu = .5$. - Fig. 7 shows the A-matrix elements a_{21} and a_{22} for $\mu = .5$. The periodicity is considerably greater than for $\mu = .2$ and a finite but still very small reverse flow effect is present but not very noticeable in fig. 7. The reverse flow is in effect for $\psi > 180^o$ (1/2 rotor rev)

and results in approximately 10% change in magnitude of the a_{22} coefficient at 3/4 of a rotor revolution. This influence is still too small to be identified accurately over 1 or 2 rotor revolutions in the presence of measurement noise. As a result the reverse flow coefficients θ_5 and θ_6 were ignored in the identification and only θ_1, θ_2 and θ_3 are identified.

Figure 8 shows the identified parameter convergence for the periodic coefficients θ_1, θ_2, and θ_3. Identification accuracy is excellent and convergence to simulation values occurs within 1 rotor revolution for the low measurement noise case. Initial parameter estimates are set to zero with large initial covariance. Convergence is rapid and excellent for all three parameter values.

Identification Results at $\mu = .8$, including reverse flow. - The coefficients of the A-matrix a_{21} and a_{22} are plotted in figure 9 for advance ratio $\mu = .8$. At this condition very strong periodicity exists including reverse flow effects. Figure 9 shows the region of reverse flow and its effect is to flatten the sine wave response for $180^0 < \psi < 360^0$ (1/2 rev. to 1 rev. of the rotor).

The parameter vector used in the identification includes all the periodic and reverse flow coefficients of the A-matrix elements a_{21} and a_{22} of Eq. (3.6) and Eq. (3.7). The parameter vector is

$$\theta^T = [\theta_1 \quad \theta_2 \quad \theta_3 \quad \theta_4 \quad \theta_5] \tag{3.12}$$

where the constant terms $\bar{a}_{21}$ and $\bar{a}_{22}$ are assumed known from the hover identification results. The identified parameter convergence is shown in figure 10 for the $\sin\psi$, $\cos\psi$ terms, figure 11 for the $\sin\psi\cos\psi$ term and figure 12 for the reverse flow coefficients θ_4 and θ_5. The periodic coefficients θ_1, θ_2 and θ_3 shown in figure 10 and figure 11 show excellent convergence as noted by the standard deviation band $\pm 1\sigma$. The reverse flow terms θ_5 and θ_6 shown in figure 12 show slow convergence as noted by the $\pm 1\sigma$ bands. The slow convergence is due to the low information content of the reverse flow coefficients which is in effect over only 1/2 of a rotor revolution. Improved accuracy can be obtained by either increasing the signal to noise ratio or averaging over many revolutions.

Figure 13 shows the parameter convergence for $\hat{\theta}_4$ and $\hat{\theta}_5$ for an increase in the signal level by a factor of 3. Convergence is better than in figure 12 as shown by the smaller $\pm 1\sigma$ bands. Parameter convergence is further shown in figure 14 for the increased signal level (x3) for a second rotor revolution using the estimated parameters and covariance at the end of the first revolution as initial estimates. Convergence is excellent after 2 rotor revolutions as shown in figure 14.

The results at advance ratio $\mu = .8$ have accurately identified the periodic coefficient model of Eq. (3.1) through Eq. (3.3), including the reverse flow terms. Since the identification is from an initial condition response the control coefficients of M_{Θ_R} shown in Eq. (3.4) are not identified. The next section discusses the results of the stochastic control application which identifies both the A-matrix elements and control matrix elements while exercising control.

Stochastic Control Results

The stochastic control formulation was briefly outlined in section II which showed the objective function for minimization (Eq. (2.3)) and the dynamic model state space description in Eq. (2.1) and Eq. (2.2). The detailed discussion of the control of systems under uncertainty, the certainty equivalence (CE) property, the caution property, and the probing property was also presented. Based upon these concepts, two cases are considered. First, the CE control is used at $\mu = 0$ and the parameter identification convergence and control performance is discussed. Second, the periodic A-matrix elements are treated as a random walk model and an assessment of the caution and probing significance is addressed.

Stochastic Control results at $\mu = 0$ using the CE controller. The CE control algorithm is shown in Eq. (2.57) through Eq. (2.59) where the parameters $\Theta(k)$ are identified on-line with the EKF. Since accurate parameter convergence requires 1/4 to 1/2 of a rotor revolution in time (.2 seconds), the control solution (Eq. (2.57)) is expected to perform less satisfactorily in the beginning and then improve as time goes on. The simulation model is shown in Eq. (3.5) where the parameter vector for identification is

$$\Theta^T = [\bar{a}_{21} \quad \bar{a}_{22} \quad \bar{b}_{21}] \tag{3.13}$$

and an initial condition $\dot{\beta} = 35$ deg/sec is used on the system.

The control objective is to minimize the criterion

$$J = E\left\{\sum_{k=1}^{N} (q_1 x_1^2(k) + q_2 x_2^2(k) + r_1 u_1^2(k)) + q_{N_1} x_1^2(N) + q_{N_2} x_2^2(N)\right. \tag{3.14}$$

where, $N = 41$, $q_1 = 0$, $q_2 = 0$, $r_1 = .2$, $q_{N_1} = 1.0$, and $q_{N_2} = .01$.

The weighting terms in the performance criterion were determined by trial and error such that the feedback was not so large as to prohibit accurate parameter

identification. The state weightings q_1 and q_2 were set to zero to permit state response of large enough magnitude for accura e parameter identification. The optimization was performed over N = 41 time steps which corresponds to 1/2 rotor revolution. The control weighting r_1 was selected to keep the control magnitude reasonably small.

Figure 15 shows the identified parameter convergence during the CE feedback control operation. The parameters are identified on-line and the controlled state response is shown in figure 16. The uncontrolled response (IC response) and the controlled response are compared in figure 16. The stability of the controlled system is increased as shown by the faster decay rate. This increased stability is further shown in figure 17, which slows the equivalent closed loop system damping parameter $a_{22_{CL}}$ ($a_{22_{CL}} = a_{22} - b_{21} L_2$). The time varying feedback gain L_2 increases significantly near the final time causing increased stability as time approachs N = 41. Note that this was dictated by selecting zero weights ($q_1 = 0$, $q_2 = 0$) on the state and nonzero weights ($q_{N_1} = 1.$, $q_{N_2} = .01$) at the terminal time. This selection permits better parameter identification to occur since the feedback is small initially and the state response is nearly that of the uncontrolled system. A time response of the control u_1 is shown in figure 18 which shows increasing control magnitude near the terminal time.

In summary, the CE control was found to accurately identify the parameters a_{21} and a_{22} while providing increased stability over the uncontrolled system. The parameter b_{21} requires further data length to improve upon accuracy. The feedback control gains were computed based upon current identified parameter estimates. The CE control was found to perform in a satisfactory manner, that is it provided increased stability for an uncertain system. The parameters of the system were identified while being controlled. Passively adaptive control proved successful for the constant coefficient system at hover.

To examine the contribution of the deterministic, caution and probing control, the performance criterion is decomposed as computed using the concepts presented in section II and ref. 26. The cost decomposition for the hover case when the model is assumed to have constant parameters is

$$J = J_{DET} + J_{PROB} + J_{CAUT} \tag{3.15}$$

where, $J_{DET} = .796$

$J_{PROB} = .012$

$J_{CAUT} = .181$

$J = .989$

As shown from the cost decomposition the probing component is negligible and caution accounts for less than 20% to the total cost J. Therefore, the control solution is dominated by the deterministic aspects of the problem and this explains the excellent performance of the CE control (probing and caution aspects are not included in the CE control design).

Stochastic control results for $\mu > 0$. - The dual control solution was investigated for this case by examination of the cost decomposition as was done at $\mu = 0$. A random walk model was assumed for the parameters to account for the periodic variation of the coefficients a_{21}, a_{22} and b_{21}. The results of the cost decomposition for the case $\mu = .8$ are shown in Eq. (3.16)

$$J = J_{DET} + J_{PROB} + J_{CAUT} \tag{3.16}$$

where, $J_{DET} = 1.92$

$J_{PROB} = .582$

$J_{CAUT} = 3.28$

$J = 5.79$

The caution component dominates the performance and is approximately 60% of the total cost. The deterministic component is nearly 30% and probing accounts for 10% of the total. These results imply that the control solution should include the caution property (the probing property can reduce the cost further, but not more than 10%).

Comparing the cost decomposition of $\mu = 0$ with $\mu > 0$ indicates that the time variation of parameters requires caution and probing properties. The larger the variation in the parameters the more dominate would be the caution and probing properties for successful identification and control.

GROUND RESONANCE PARAMETER IDENTIFICATION

The results of application of parameter identification to helicopter ground resonance is presented in this section. The EKF is used as the parameter identification method and results of a multiblade coordinate measurement model is assumed as well as a single blade measurement. The single blade measurement results in periodic coefficients in the measurement equations.

Ground Resonance Model Description

The parameter identification objective is to identify the rotor blade damping and thus, using a linearized multiblade coordinate model, the system modal damping (eigenvalues) can be determined. This differs from the modal damping determination technique of ref. 35 which determines the modal damping directly using the moving-block Fast Fourier Transform (FFT) approach. In ref. 7 modal damping is determined from random responses. The advantage of the state space approach is that the blade damping, η_ζ can be identified at a lower RPM condition (i.e. before coalescence with support frequency). Then, stability (eigenvalues) can be predicted at all RPM conditions before testing at these conditions. This capability permits considerable safety in testing new rotor designs. The modal damping identification techniques of ref. 35 and ref. 7 can only be applied at the RPM condition under test (i.e. prediction capability is not possible).

The second order equations of motion for the ground resonance description include multiblade rotor coordinates ζ_{1c} and ζ_{1s} for rotor lag degree of freedom and the support x and y degrees of freedom. The model is shown in Eq. (3.17) and is representative of a full scale rotor system being tested on a wind tunnel support system.

$$\begin{bmatrix} 1 & 0 & 0 & 1.5 \\ 0 & 1 & -1.5 & 0 \\ 0 & -.001 & 1 & 0 \\ .001 & 0 & 0 & 1 \end{bmatrix} \begin{bmatrix} \ddot{\zeta}_{1c} \\ \ddot{\zeta}_{1s} \\ \ddot{x} \\ \ddot{y} \end{bmatrix} + \begin{bmatrix} 2\bar{\omega}_\zeta\eta_\zeta & 2 & 0 & 0 \\ -2 & 2\bar{\omega}_\zeta\eta_\zeta & 0 & 0 \\ 0 & 0 & 2\bar{\omega}_x\eta_x & 0 \\ 0 & 0 & 0 & 2\bar{\omega}_y\eta_y \end{bmatrix} \begin{bmatrix} \dot{\zeta}_{1c} \\ \dot{\zeta}_{1s} \\ \dot{x} \\ \dot{y} \end{bmatrix}$$

$$+ \begin{bmatrix} (\bar{\omega}_\zeta^2-1) & +2\bar{\omega}_\zeta\eta_\zeta & 0 & 0 \\ -2\bar{\omega}_\zeta\eta_\zeta & (\bar{\omega}_\zeta^2-1) & 0 & 0 \\ 0 & 0 & \bar{\omega}_x^2 & 0 \\ 0 & 0 & 0 & \bar{\omega}_y^2 \end{bmatrix} \begin{bmatrix} \zeta_{1c} \\ \zeta_{1s} \\ x \\ y \end{bmatrix} = \begin{bmatrix} 0 \\ 0 \\ \bar{F}_x \\ \bar{F}_y \end{bmatrix} \qquad (3.17)$$

These equations result from the original derivation by Coleman [36] and are also developed in ref. 37. Ground resonance is of concern when the rotor RPM, Ω is such that the inplane regressing frequency coalesces with the support degrees of freedom. This can result in an instability and is thus a concern during helicopter wind tunnel tests of new rotor designs.

Two measurement systems are addressed. The multiblade measurement model assumes measurement of ζ_{1c}, ζ_{1s}, x, y (i.e. each degree of freedom). The single blade measurement model is

$$\zeta = \zeta_{1c} \cos\psi + \zeta_{1s} \sin\psi \tag{3.18}$$

and also includes the support positions x and y.

The nominal parameter values for support and rotor degrees of freedom are

$$\begin{aligned} \omega_x &= 11.6 \text{ rad/sec} \qquad \bar{\omega}_\zeta = .3 \\ \omega_y &= 14.6 \text{ rad/sec} \qquad \eta_\zeta = .03 \\ \eta_x &= .04 \\ \eta_y &= .04 \end{aligned} \tag{3.19}$$

The continuous in time state variable description of the ground resonance model is shown in Eq. (3.20) and Eq. (3.21).

$$\dot{x} = Ax + Bu \tag{3.20}$$

$$y = Cx \tag{3.21}$$

The state, control and nonrotating measurements are defined as

$$x = \begin{bmatrix} \zeta_{1c} \\ \zeta_{1s} \\ \bar{x} \\ \bar{y} \\ \dot{\zeta}_{1c} \\ \dot{\zeta}_{1s} \\ \dot{\bar{x}} \\ \dot{\bar{y}} \end{bmatrix}, \quad u = \begin{bmatrix} F_x \\ F_y \end{bmatrix}, \quad y = \begin{bmatrix} \zeta_{1c} \\ \zeta_{1s} \\ \bar{x} \\ \bar{y} \end{bmatrix} \tag{3.22}$$

The rotating measurements and support coordinates are

$$y = \begin{bmatrix} \zeta \\ \bar{x} \\ \bar{y} \end{bmatrix} \tag{3.23}$$

The A and B matrices can be expressed in terms of RPM (Ω) and inplane damping η_s as follows.

$$
A = \left[\begin{array}{cccc|cccc}
0 & 0 & 0 & 0 & 1.0 & 0 & 0 & 0 \\
0 & 0 & 0 & 0 & 0 & 1.0 & 0 & 0 \\
0 & 0 & 0 & 0 & 0 & 0 & 1.0 & 0 \\
0 & 0 & 0 & 0 & 0 & 0 & 0 & 1.0 \\
\hline
+ .9114 & - .6009\eta_\zeta & 0 & + \frac{320.2196}{\eta^2} & - .6009\eta_\zeta & -2.003 & 0 & + \frac{1.7546}{\Omega} \\
+ .6009\eta_\zeta & + .9114 & - \frac{202.1428}{\Omega^2} & 0 & +2.003 & - .6009\eta_\zeta & - \frac{1.3941}{\Omega} & 0 \\
+6.009\times10^{-4}\eta_\zeta & +9.1137\times10^{-4} & - \frac{134.7618}{\Omega^2} & 0 & +2.003\times10^{-3} & -6.009\times10^{-4}\eta_\zeta & - \frac{.9294}{\Omega} & 0 \\
-9.1137\times10^{-4} & +6.009\times10^{-4}\eta_\zeta & 0 & - \frac{213.4797}{\Omega^2} & +6.009\times10^{-4}\eta_\zeta & +2.003\times10^{-3} & 0 & - \frac{1.1698}{\Omega}
\end{array}\right]
\tag{3.24}
$$

$$B = \begin{bmatrix} 0 & 0 \\ 0 & 0 \\ 0 & 0 \\ 0 & 0 \\ 0 & -\frac{3.0570\times10^{-5}}{\Omega^2} \\ \frac{2.7146\times10^{-5}}{\Omega^2} & 0 \\ \frac{1.8097\times10^{-5}}{\Omega^2} & 0 \\ 0 & \frac{2.0381\times10^{-5}}{\Omega^2} \end{bmatrix} \tag{3.25}$$

The nonrotating measurement matrix is

$$C = \begin{bmatrix} 1 & 0 & 0 & 0 & 0 & 0 & 0 & 0 \\ 0 & 1 & 0 & 0 & 0 & 0 & 0 & 0 \\ 0 & 0 & 1 & 0 & 0 & 0 & 0 & 0 \\ 0 & 0 & 0 & 1 & 0 & 0 & 0 & 0 \end{bmatrix} \tag{3.26}$$

The single blade rotating measurement and support measurement matrix is

$$C = \begin{bmatrix} \cos\psi & \sin\psi & 0 & 0 & 0 & 0 & 0 & 0 \\ 0 & 0 & 1 & 0 & 0 & 0 & 0 & 0 \\ 0 & 0 & 0 & 1 & 0 & 0 & 0 & 0 \end{bmatrix} \tag{3.27}$$

The state equations defined in Eq. (3.20) through (3.27) are used in discrete form in the identification.

The eigenvalues for four selected conditions are obtained from the A matrix of Eq. (3.24). The four conditions yield either a stable or unstable condition depending on the value of rotor rotational speed (Ω) and blade inplane damping (η_L). The four conditions selected are;

CASE	Ω(RPM)	η_s	COMMENTS
1	150	.03	Stable
2	150	.02	Stable
3	160	.03	Stable
4	160	.02	Unstable

The complete eigenvalues are shown in Table 3.

For ground resonance detection, it is desirable to identify and monitor continuously the stability as RPM is increased. Cases 1 and 3 represents a stable situation and cases 2 and 4 represents a change from a stable to an unstable situation. The stable-to-unstable situation could be predicted without testing at the unstable condition if blade damping was identified at case 2 (Ω = 150 RPM) and then eigenvalues obtained from the A-matrix (Eq. 3.24) for Ω = 160 RPM. This prediction capability is a primary advantage of the state space approach over the modal approach of ref. 7 and ref. 35.

Use of Free Response Data for Identification of Damping for Ground Resonance.- The original goal of this research activity was to utilize the dual property of stochastic control to enhance identification of parameters. The emphasis of the ground resonance study was toward the identification aspects. Simulations were performed using the dual control solution and it was concluded that the dual control solution required excessive control magnitudes for the system modeled by Eq. (3.17) and Eq. (3.19). The magnitude of the available control is found to be too constrained in magnitude so that the dual control cannot be effective in producing a significant response over small time intervals.

Since, the main emphasis of the ground resonance study is on the parameter identification aspects, it was decided that identification from free response data or open loop forced response data would be a more effective solution for the ground resonance problem. Thus, all results presented are from free response data for the ground resonance problem.

Numerous simulations were performed using the ground resonance math model. A sample time of Δt = .005 was found to yield accurate results and thus all simulations were performed with this sample time. In addition, all simulation runs were performed at a RPM of Ω = 150 and blade in-plane damping of η_ζ = .03. This represents a lightly damped case and is representative of a typical condition for which parameter identification is important.

All identification runs were performed from simulated initial condition free response data. Five different initial condition sets were investigated shown in Table 4.

Initial condition set 1 was an arbitrary guess, whereas initial condition set 2 through set 4 was obtained by simulation of the ground resonance model with sine input forcing on F_x. Initial condition set 2 through set 4 was obtained from the forced state response at different time points. This procedure closely resembles that used to generate free response data using stick stirring for flight and wind tunnel testing. Initial condition set 5 was obtained by applying an impulse to the F_x control input and computing the state variable response at t = 0+. Figure 19 through figure 24 shows the state response ζ_{1c}, ζ_{1s}, x and y and measurements ζ for IC set 2, 3 and 5. All figures show 150 time steps (.75 secs).

Random measurement noise was added to all measurements and three different noise sequence sets were investigated. The noise levels for the constant and periodic model are as follows.

Standard Deviation of Measurement Noise (constant Coeff. Model)			Standard Deviation of Measurement Noise (periodic Coeff. Model)		
ζ_{1c}	rad	5.3×10^{-4}	ζ	rad	5.3×10^{-4}
ζ_{1s}	rad	5.3×10^{-4}	x	- *	3.9×10^{-5}
x	- *	3.9×10^{-5}	y	- *	3.9×10^{-5}
y	- *	3.9×10^{-5}			

* Nondimensional (÷ R)

The noise levels were selected such that 3σ was approximately 10% of the signal level. For example, for an assumed blade lag response of 1 degree (.017 rad.), $3\sigma_\zeta = 15.9\times10^{-4}$ is approximately 10% of lag response.

Two different initial starting estimates for the blade lag damping were used. A initial estimate $\hat{\eta}_\zeta = .04$ was selected to be close to the true parameter used in the simulation ($\eta_{True} = .03$). An initial damping estimate of $\hat{\eta}_\zeta = .1$ was used to represent an initial guess far removed from the simulation value.

Parametric studies were performed using the conditions outlined above to study parameter identification convergence for blade damping.

Parameter Identification Results

This section shows the results of parameter identification from the ground resonance simulation model which was outlined in the last section. All computer runs were performed at 150 RPM and blade inplane damping $\eta_\zeta = .03$. The identification runs were performed using up to a maximum of .75 seconds of data (approximately 2 rotor revolutions) at a sample interval of $\Delta t = .005$ sec. The lightly damped mode has a frequency of 11.07 rad/sec ($.707\Omega$) and thus .75 seconds of data is approximately 1 1/2 cycles of this mode.

The results are presented in Figure 25 through Figure 33. Table 5 is presented for convenience which summarizes the conditions used for each run presented in the figures. Each figure will be discussed separately with reference to Table 5.

Figure 25 shows identified damping convergence for three different random measurement noise sequences. Initial condition set 1 (the arbitrary guess) is used and the parameter process noise covariance $Q^\Theta = 0$. The top figure shows the results for the three noise sequences for only 40 samples (.2 secs). The bottom figure is a continuation for noise sequence set 3 and is shown for 80 samples (.4 sec). The initial parameter starting value is $\hat{\eta}_\zeta = .04$ and is close to the true value of $\eta_\zeta = .03$. Convergence is good for all three noise sets and requires 80 samples or more for convergence as shown by the bottom figure.

Figure 26 shows identified damping for three different initial condition sets ($Q^\Theta = 0$). Initial condition set 5 has more information content for improved identifibility whereas IC set 2 has less information content thus convergence is slower. The rate of convergence is reflected in the covariance of the estimate ($\pm 1\sigma$ is shown in the figure). The convergence of IC set 4 (denoted by the circle) has falsely converged to .042 because the estimate of the damping has deviated far from the true value resulting in violation of linearizations in the E.K. IC set 4 is an example of poor convergence as discussed in section 2.0 because the process noise covariance $Q^\Theta = 0$. IC set 2 and IC set 5 show acceptable convergence.

Figure 27 shows identified parameter convergence comparing the constant and the periodic coefficient measurement model. Again the initial damping $\hat{\eta}_\zeta = .04$ and $Q^\Theta = 0$. Convergence is good in both cases with the constant coefficient model showing fater convergence. A longer data record is required for the periodic model.

Figure 28 through Figure 33 use an initial parameter estimate of $\hat{\eta}_\zeta = .1$ which is far removed from the simulation value of $\eta_\zeta = .03$. The constant coefficient model results are shown in Figure 28 ($Q^\Theta = 0$) and Figure 29 ($\Theta^\Theta \neq 0$). False convergence is shown in Figure 28 with $Q^\Theta = 0$, whereas good convergence is shown in Figure 29 with $Q^\Theta \neq 0$. The $\pm 2\sigma$ uncertainty bands in the figures reflect convergence.

Figure 30 and Figure 31 show results for the periodic coefficient model for $Q^\Theta = 0$ and $Q^\Theta \neq 0$, respectively. The results are similar to the constant coefficient case of Figures 28 and 29. Excellent convergence is shown in Figure 31 which uses $Q^\Theta \neq 0$. IC set 5 is used with .75 seconds (150 samples of data).

Figure 32 shows results for the periodic measurement model with initial condition set 2 obtained from stick stirring. Convergence is acceptable as determined by the $\pm 2\sigma$ band shown in the figure with $Q^\Theta \neq 0$. Convergence to the true parameter value requires a longer data record.

Figure 33 shows results for the periodic measurement model with IC set 3 also obtained from stick stirring. IC set 3 was selected after allowing a further increase in the time over IC set 2 before setting the control input to zero. The initial conditions thus obtained yield better information for the resulting free response data. Therefore, identified parameter convergence is faster for IC set 3 over IC set 2. This is reflected in the $\pm 2\sigma$ band shown in the figures. Convergence is excellent as shown in Figure 33.

Figure 33 demonstrates that parameter identification of inplane blade damping is possibl using less than 1 second of data (approximately 2 rotor revolutions) using a single blade measurement of blade angle in the rotating system (periodic measurement model) and x and y support position measurements.

A summary of main conclusions for the ground resonance study is as follows;

- The use of free response data for identification of the in-plane damping parameter has been shown to yield excellent convergence using stick stirring to obtain initial conditions.
- Excellent parameter identification of damping was shown for both the constant and periodic measurement model.
- The extended Kalman filter (for the no process noise case) has shown excellent identified parameter convergence (providing the process noise covariance on the parameter, Q^Θ, is set to a nonzero value).
- The state variable multiblade model A-matrix can be used to predict the stability for RPM conditions before they are tested. This feature makes this approach to identification very competative with the modal approach of ref. 35 and ref. 7.

CONCLUSIONS

A general procedure for parameter identification and stochastic control of helicopter rotor dynamic systems has been presented. The formulation is based upon a state variable representation described by constant and periodic coefficients. The extended Kalman filter was shown to yield unbiased parameter estimates for all case studies for both periodic and constant coefficient models. This was found to be true for systems without process noise.

The pure identification results of the rotor flap model were successful over an advance ratio of $\mu = 0$ to $\mu = .8$. This included constant and periodic coefficients and the effects of reverse flow. Typically less than 1 rotor revolution was required where there was sufficient signal to noise ratio. Stochastic control of the rotor flap model was successful in that stability was improved while parameters were accurately identified. The CE control was found to be successful at $\mu = 0$. For systems with time varing coefficients, the caution property was found to dominate, with the probing property contributing 10% to the total cost function.

Pure identification was successful for the ground resonance problem for either the multiblade coordinate rotor inplane measurement model or for a single rotating blade measurement. Typically 2 rotor revolutions are required in 10% measurement noise where free-response data is used (generated from a stick stirring control input). The state variable identification approach has the advantage over modal methods (e.g. the moving-block FFT method) in that stability prediction over the complete RPM range is possible from test data obtained at one test RPM condition.

The EKF identification method is an efficient identification approach for systems without process noise. The "corrected" EKF (Ljung 1979) should be investigated for systems with both measurement and process noise. The corrected EKF method could be assessed via simulation and test data applications.

The rotor flap model investigated in this study could be extended to include blade inflow models and higher degrees of blade flexibility. Identification of periodic coefficient models should include a hypothesis testing procedure (e.g. stepwise multiple regression) for automatic determination of the required periodic terms in the model. This is important since, in general, it is not known which periodic terms would be required, particularly in the reverse flow region. The

identification and stochastic control methods u d in this research should be investigated as to more efficient computational algorithms, which is of particular importance for real time or near real time applications.

APPENDIX A

AUTOMATIC CALCULATION OF THE JACOBIAN

The Extended Kalman Filter is quite similar to the standard Kalman Filter with the exception of the need to evaluate the Jacobian (2.19) at every step.

In practice the unknown parameters appear in several elements of the continuous time system matrices $A(\Theta)$ and $B(\Theta)$ from (2.4). Furthermore, a particular parameter usually appears in several elements of the system matrices.

The following procedure, applicable for a wide class of problems, can be used to automate the calculation of the Jacobian.

It is assumed that the system matrices A and B from (2.4) have elements a_{ij} and b_{ij} that are either known or given by the product of a known constant with an unknown parameter. To indicate which parameters enter where in A and B define the matrices

$$A^P = [a^P_{ij}] \tag{A.1}$$

$$B^P = [b^P_{ij}] \tag{A.2}$$

of dimensions $n_x x n_x$ and $n_x x n_u$, respectively, where

$$a^P_{ij} = \begin{cases} 0 \text{ if } a_{ij} = \bar{a}_{ij} \\ m \text{ if } a_{ij} = \bar{a}_{ij}\Theta_m \end{cases} \tag{A.3}$$

where $1 \leq m \leq n_\Theta$ and

$$\bar{A} = [\bar{a}_{ij}] \tag{A.4}$$

is a known matrix and similarly for b^P_{ij}.

Thus

$$a_{ij} = \begin{cases} \bar{a}_{ij} & \text{if} \quad a^P_{ij} = 0 \\ \bar{a}_{ij}\Theta_m & \text{if} \quad m \triangleq a^P_{ij} \neq 0 \end{cases} \tag{A.5}$$

Propagation of the state (2.15) requires the evaluation of

$$f[\hat{z}(k|k),\ u(k)] = \begin{bmatrix} F(\hat{\Theta}(k|k))\hat{x}(k|k) + G(\hat{\Theta}(k|k))u(k) \\ \\ \hat{\Theta}(k|k) \end{bmatrix} \tag{A.6}$$

which, in turn, requires the evaluation of $F(\hat{\Theta}(k|k))$. The latter can be then easily obtained based on (A.5) as

$$F(\hat{\Theta}(k|k)) = I + A(\hat{\Theta}(k|k))\Delta \tag{A.7}$$

with

$$a_{ij}(\hat{\Theta}(k|k)) = \begin{cases} \bar{a}_{ij} & \text{if} \quad a_{ij}^{p} = 0 \\ \\ \bar{a}_{ij}\hat{\Theta}_{m}(k|k) & \text{if} \quad m \triangleq a_{ij}^{p} \neq 0 \end{cases} \tag{A.8}$$

The covariance propagation equation (2.18) requires the evaluation of the Jacobian (2.19) which is an $n_z x n_z$ matrix. Based on (A.1)-(A.4) the expressions of the elements of the Jacobian matrix

$$\Phi(k) = [\Phi_{ij}(k)] \tag{A.9}$$

are

$$\Phi_{ij}(k) = F_{ij}(\hat{\Theta}(k\ k)) \qquad i=1,\ldots,n_x\ ;\ j=1,\ldots,n_x \tag{A.10}$$

$$\Phi_{ij}(k) = 1 \qquad i=j=n_x + m\ ;\ m=1,\ldots,n_\Theta \tag{A.11}$$

$$\Phi_{i,n_x+m}(k) = \left(\sum_{\ell \in L^a(i,m)} \bar{a}_{i\ell}\ \hat{x}_\ell(k|k) + \sum_{\ell \in L^b(i,m)} \bar{b}_{i\ell}\ u_\ell(k) \right) \Delta$$

$$i = 1,\ldots,n_x\ ;\ m = 1,\ldots,n_\Theta \tag{A.12}$$

$$\Phi_{ij}(k) = 0 \qquad \text{otherwise} \tag{A.13}$$

where

$$L^a(i,m) = \{\ell\ :\ a_{i\ell}^{p} = m\} \tag{A.14}$$

is the set of state components that multiply Θ_m in the i-th row of (2.12) and

$$L^b(i,m) = \{\ell : b^p_{i\ell} = m\} \tag{A.15}$$

is the set of control components that multiply Θ_m in the i-th row of (2.12).

In a similar manner one can compute the Hessian of f_ℓ, the ℓ-th component of the vector valued function f from (2.12), denoted as

$$\psi^\ell = \left[\psi^\ell_{ij}\right] \triangleq f_{\ell,zz} = \left[\frac{\partial^2 f_\ell}{\partial z_i \, dz_j}\right] \tag{A.16}$$

The expression of the elements of this symmetric matrix is

$$\psi_{n_x+m,i} = \psi^\ell_{i,n_x+m} = \begin{cases} \bar{a}_{\ell i}\ \Delta \text{ if } \ a^p_{\ell i} = m \ \text{ for } i = 1,\ldots,n_x \ ; \ m = 1,\ldots,n_\Theta \\ \\ 0 \quad \text{Otherwise} \end{cases} \tag{A.17}$$

References

1. Molusis, J.A., Rotorcraft Derivative Identification From Analytical Models and Flight Test Data, AGARD Conference Proceedings No. 172 on Methods for Aircraft State and Parameter Identification, May 1975.

2. Gould, D.G. and Hindson, W.S., Estimates of the Stability Derivatives of a Helicopter and a V/STOL Aircraft from Flight Data, AGARD Conference Proceedings No. 172 on Methods for Aircraft State and Parameter Identification, May 1975.

3. Hall, W.E., Jr., Grupta, N.K. and Hansen, R.S., Rotorcraft System Identification Techniques for Handling Qualities and Stability and Control Evaluation, 34th Forum of the American Helicopter Society, Wash. D.C., May 1978.

4. Padfield, G.D. and Duval, R.W., Applications of Parameter Estimation Methods to the Prediction of Helicopter Stability, Control, and Handling Characteristics, NASA Conference Publication 2219, Proceedings of a Specialists Meeting on Helicopter Handling Qualities, April 14-15, 1982.

5. Hohenemser, K.H. and Prelewicz, D.A., Computer Experiments on Periodic Systems Identification Using Rotor Blade Transient Flapping-Torsion Responses at High Advance Ratio, AHS/NASA-Ames Specialists' Meeting on Rotorcraft Dynamics, Feb. 1974.

6. Kanning, G. and Biggers, J.C., Application of a Parameter Identification Technique to a Hingless Helicopter Rotor. NASA TN D-7834, Dec. 1974.

7. Molusis, J.A., Rotorcraft Blade Mode Damping Identification from Random Responses Using a Recursive Maximum Likelihood Algorithm, NASA-CR 3600, Sept. 1982.

8. Hall. W.E., Jr. and Bryson, A.E., Jr., Inclusion of Rotor Dynamics in Controller Design for Helicopters, Jour. of Aircraft, Vol. 10, No. 4, April 1973.

9. Briczinski, S.J., Analytical Investigation of Gust Suppresion Techniques for the CH-53 Helicopter, NASA-CR-145013, 1976.

10. Briczinski, S.J. and Copper, D.E., Flight Investigation of Rotor/Vehicle State Feedback, NASA CR-132546, 1975.

11. Taylor, R.B., Zwicke, P.E., Gold, P., and Miao, W., Analytical Design and Evaluation of an Active Control System for Helicopter Vibration Reduction and Gust Response Alleviation, NASA CR-152377, 1980.

12. Molusis, J.A., Hammond, C.E., and Cline, J.H., A Unified Approach to the Optimal Design of Adaptive and Gain Scheduled Controllers To Achieve Minimum Helicopter Rotor Vibration, 37th Forum Proceedings of the American Helicopter Society, May 17-20, 1981.

13. Shaw, J., and Albion, N., Active Control of the Helicopter Rotor for Vibration Reduction, 36th Annual Forum of the American Helicopter Society, May 1980.

14. Johnson, W., Self-Tuning Regulators for Multicyclic Control Of Helicopter Vibration, NASA Technical Paper 1996, March 1982.

15. Chopra, I. and McCloud, III, J.L., Considerations of Open-Loop, Closed-Loop, and Adaptive Multicyclic Control Systems, AHS Specialists' Meeting on Helicopter Vibration, Hartford, Conn., Nov. 1981.

16. Kretz, M., Active Elimination of Stall Conditions, 37th Forum Proceedings of the American Helicopter Society, May 17-20, 1981.

17. Ham, N.D. and Quackenbush, T.R., A Simple System for Helicopter Individual Blade Control and Its Application to Stall Induced Vibration Alleviation, AHS Specialists' Meeting on Helicopter Vibration, November 1981.

18. Guinn, K.F., Individual Blade Control Independent of a Swashplate, Jour. of the American Helicopter Society, Vol. 27-No. 3, July 1982.

19. Bar-Shalom, Y. and Tse, E., Concepts and Methods in Stochastic Control, in Control and Dynamic Systems: Advances on Theory and Applications, C.T. Leondes (ed.), Academic Press, 1976.

20. Soderstrom, T., Ljung, L. and Gustavsson, I., A Comparative Study of Recursive Identification Methods, Lund Institute of Technology Dept. of Automatic Control, Report 7427, Dec. 1974.

21. Ljung, L., Asymptotic Behavior of the Extended Kalman Filter as a Parameter Estimator for Linear Systems, IEEE Transaction on Automatic Control, Vol. AC-24, No. 1, Feb. 1979.

22. Mehra, R.K., Identification of Stochastic Linear Dynamic Systems Using Kalman Filter Representation, AIAA Journal, Vol. 9, No. 1, Jan. 1971.

23. Maine, R.E. and Iliff, K.W., Formulation of a Practical Algorithm for Parameter Estimation with Process Noise and Measurement Noise, Proceedings of the Sixth IFAC Symposium on Identification and System Parameter Estimation, Vol, 2, Arlington Va., June 7-11, 1982.

24. Bar-Shalom, Y., Stochastic Dynamic Programming, Caution and Probing, IEEE Trans. Automat. Contr., AC-26, 1184-1195, 1981.

25. Feldbaum, A., Optimal Control Systems, Academic Press, 1965.

26. Bellman, R. Dynamic Programming, Princeton Univ. Press, 1957.

27. Raiffa, H., Schlaifer, Applied Statistical Decision Theory, MIT Press, 1972.

28. Bar-Shalom, Y., Tse, E., Dual effect, certainty equivalence, and separation in stcchastic control, IEEE Trans. Automat. Contr., AC-19, 494-500, 1974.

29. Speyer, J., Deyst, J., and Jacobson, D., Optimization of stochastic linear systems with additive measurement and process noise using exponential performance criteria, IEEE Trans. Automat., Contr., AC-19, 358-366, 1974.

30. Åström, K. J., Borisson, U., Ljung, L., Wittenmark, B., Theory and application of self-tuning regulators, Automatica, 13, 457-476, 1977.

31. Bryson, A.E. and Ho, Yu-Chi, Applied Optimal Control, Blaisdell Publishing Co., 1969.

32. Tse, E., Bar-Shalom, Y., and Meier, L., Wide-sense adaptive dual control of stochastic nonlinear systems, IEEE Trans. Automat. Contr., AC-18, 98-108, 1973.

33. Tse, E., Bar-Shalom, Y., An actively adaptive control for discrete-time systems with random parameters, IEEE Trans. Automat. Contr., AC-18, 109-117, 1973.

34. Taylor, J.R., The Cramer-Rao Estimation Error Lower Bound Computation for Deterministic Nonlinear Systems, IEEE Transaction on Automatic Control, Vol. AC-27, No. 2, April, 1979.

35. Warmbrodt, W. and McCloud, J., Full-Scale Wind-Tunnel Test of the Aeroelastic Stability of a Bearingless Main Rotor, Proceedings of the 37th Annual Forum of the American Helicopter Society, May 17-20, 1981.

36. Coleman, R.P., and Feingold, A.M., Theory of Self-Excited Mechanical Oscillations of Helicopter Rotors with Hinged Blades, NACA Report 1351, 1958.

37. Hammond, C.E., An Application of Floquet Theory to Prediction of Mechanical Instability, Presented at the AHS/NASA Ames Specialists' Meeting on Rotorcraft Dynamics, Feb. 13-15, 1974.

38. Johnson, Wayne, Helicopter Theory, Princeton University Press, 1980.

Table 1. - Identification Methods Which Yield Asymptotically Unbiased Estimates

NOISE TYPE	BATCH (OFF-LINE)	RECURSIVE (ON-LINE)
PROCESS NOISE	• LEAST SQUARES (LS) (EQUATION ERROR)	• RLS
MEASUREMENT NOISE	• MAXIMUM LIKELIHOOD (ML) (OUTPUT ERROR)	• RML • EXTENDED KALMAN FILTER (EKF)
PROCESS AND MEASUREMENT	• MAXIMUM LIKELIHOOD (ML) (PREDICTION ERROR)	• RML (Soderstrom 1973) • CORRECTED EKF (Ljung 1979)

Table 2. - Flap Equation Periodic Coefficient Va'ues with Advance Ratio

$\bar{a}_{21} = -5.61$

$\bar{a}_{22} = .895$

A-MATRIX ELEMENT	ADVANCE RATIO	θ_1	θ_2	θ_3	θ_4	θ_5
a_{12}	0	.0	-	.0	.0	-
	.2	.935	-	.2807	.00748	-
	.5	2.339	-	1.754	.2924	-
	.8	3.743	-	4.491	1.916	-
a_{22}	0	-	.0	-	-	.0
	.2	-	.0279	-	-	.000111
	.5	-	.0698	-	-	.00436
	.8	-	.1117	-	-	.02859

Reverse Flow

ORIGINAL PAGE IS OF POOR QUALITY

Table 3. - Eigenvalues for Ground Resonance Model (Frequency Nondimensioned by Ω)

Case 1	Case 2
$\Omega = 150,\ \eta_\zeta = .03$	$\Omega = 150,\ \eta_\zeta = .02$
$-.00969 \pm j\ 1.307$	$-.00669 \pm 1.307$
$-.0368 \pm j\ .925$	$-.0368 \pm .925$
$-.0059 \pm j\ .705$	$-.0027 \pm .705$
$-.0324 \pm j\ .731$	$-.0325 \pm .732$

Case 3	Case 4
$\Omega = 160,\ \eta_\zeta = .03$	$\Omega = 160,\ \eta_\zeta = .02$
$-.00955 \pm j\ 1.307$	$-.00654 \pm j\ 1.307$
$-.0346 \pm j\ .867$	$-.0346 \pm j\ .867$
$-.0012 \pm j\ .699$	$+.0012 \pm j\ .694$
$-.0352 \pm j\ .692$	$-.0346 \pm j\ .692$

Table 4. - Initial Condition Sets Used to Generate Free Response Data for Ground Resonance Identification

State	Units	IC Set 1	IC Set 2	IC Set 3	IC Set 4	IC Set 5
ζ_{1c}	Rad.	.01	.0139	-.0187	.0118	.0
ζ_{1s}	Rad.	.017	.00264	.0181	-.0251	.0
x	- *	.0012	.0000889	-.00134	.0012	.0
y	- *	-.001	.0000198	-.000011	.0	.0
$\dot{\zeta}_{1c}$	Rad/Sec	.0	-.0197	-.217	.274	.0
$\dot{\zeta}_{1s}$	Rad/Sec	.0	.164	-.217	.122	.135
$\dot{x}$	1/sec *	.0125	-.007	-.00553	.0107	.09
$\dot{y}$	1/sec *	0	.0000562	-.000358	.00055	.0

* Nondimensional (÷ R)

Notes: IC set 1 obtained from arbitrary guess.

IC set 2 through 4 obtained from stick stirring.

IC set 5 obtained from pulse input.

Table 5. - Parameter Identification Run Summary for Ground Resonance Study

Figure Number	Constant or Periodic Model	Initial Parameter Estimate $\hat{\eta}_\zeta$	Initial Condition Set No.	Noise Sequence No.	Parameter Process Noise Q^θ	Comments
25	Constant	.04	1	1,2,3	0	. Shows effect of Noise Sequence
26	"	"	2,4,5	3	0	. Shows IC's, False Convergence
27	Constant Vs Periodic	"	5	↓	0	. Constant Vs Periodic for close initial $\hat{\eta}_s$
28	Constant	.1	5	↓	0	. False Convergence with $Q^\theta = 0$
29	"	↓	5	↓	$\neq 0$	. Good Convergence with $Q^\theta \neq 0$
30	Periodic	↓	5	↓	0	. False Convergence with $Q^\theta = 0$
31	↓	↓	5	↓	$\neq 0$	. Good Convergence with $Q^\theta \neq 0$
32	↓	↓	2	↓	$\neq 0$	. IC set 2 from stick stirring, proper convergence but requires more data
33	↓	↓	3	↓	$\neq 0$	. IC set 3 from stick stirring, good convergence

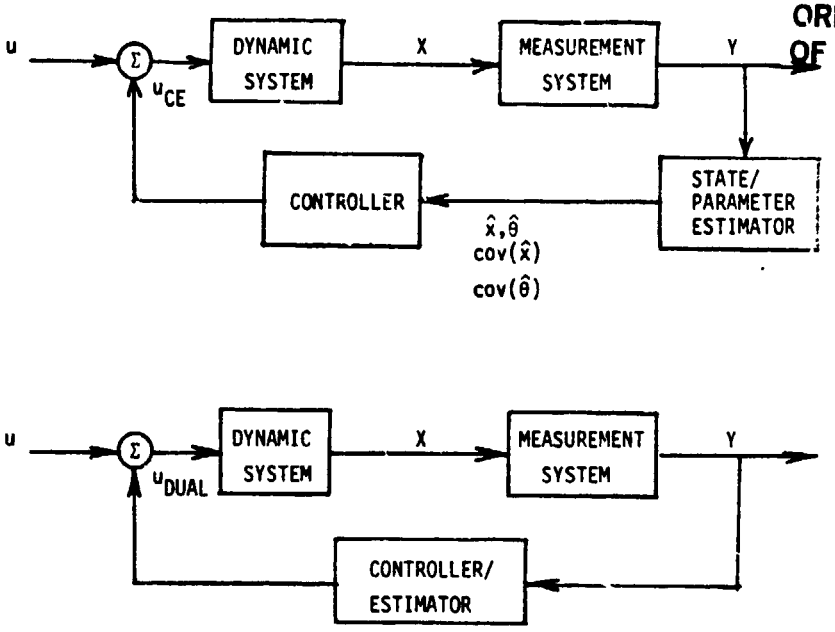

Figure 1. - Stochastic Controllers Based upon the Certainty Equivelance Property and the Dual Property of Stochastic Control Theory.

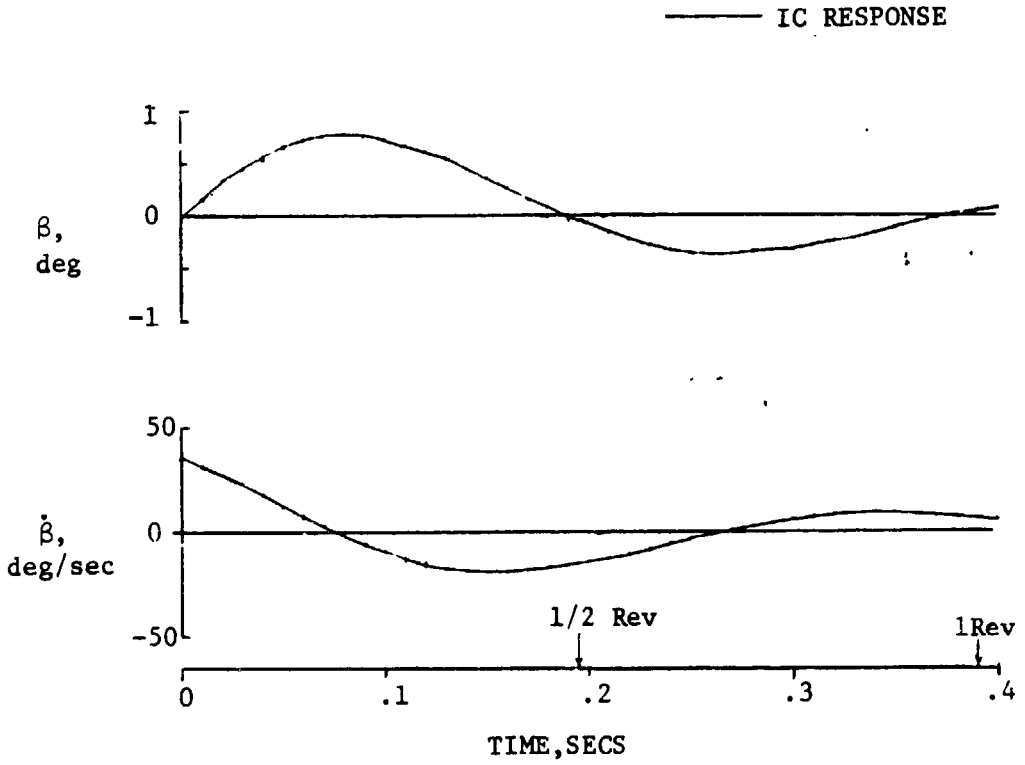

Figure 2. - Rotor Flap Model State Time History Response Obtained From Free Response Portion of Pulse Input. ($\dot{\beta}(0)$ = 35 deg/sec).

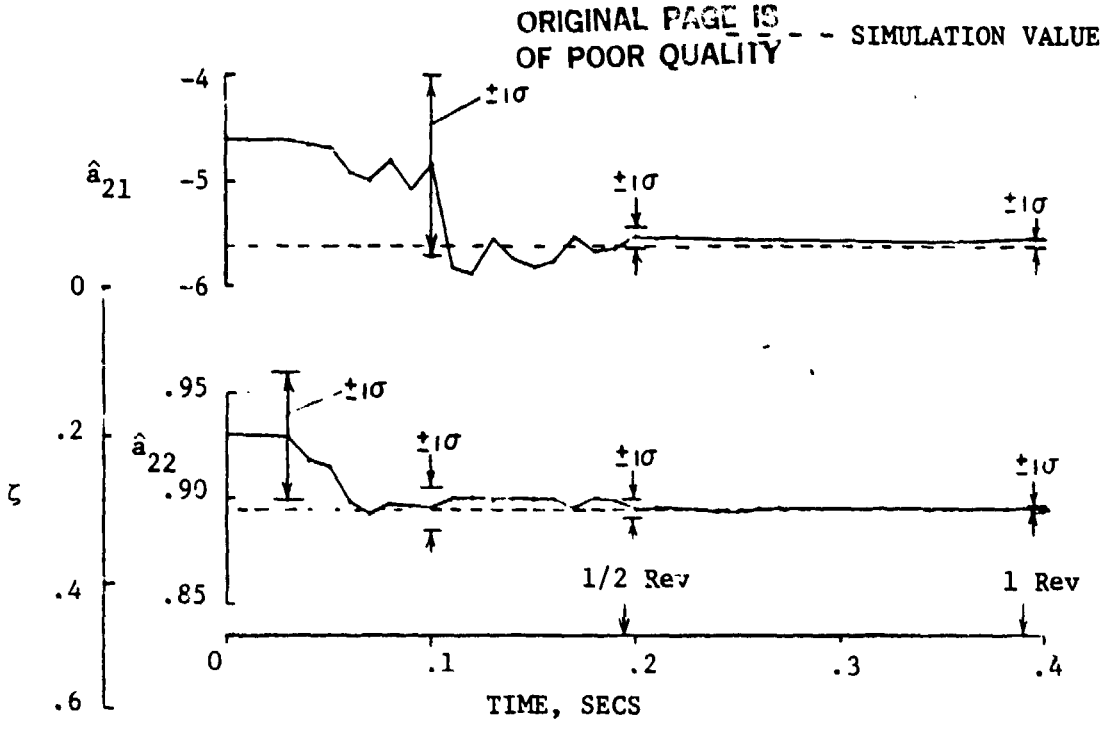

Figure 3. - Rotor Flap Model Identified Parameter Convergence, μ = 0 (No Periodicity, High Noise).

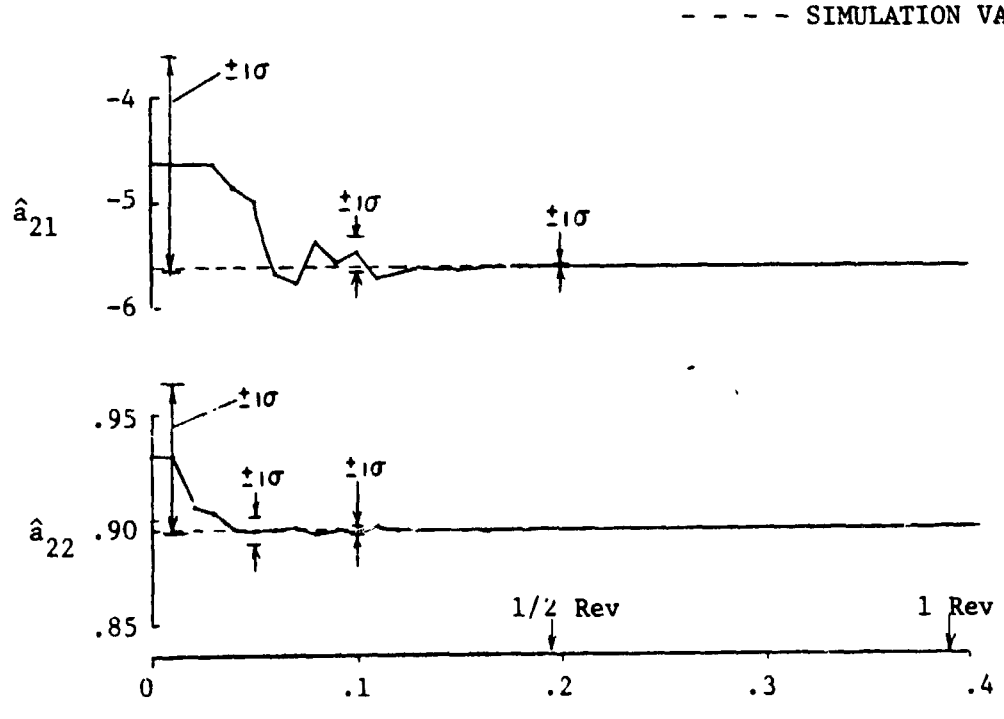

Figure 4. - Rotor Flap Model Identified Parameter Convergence, μ = 0 (No Periodicity, Low Noise).

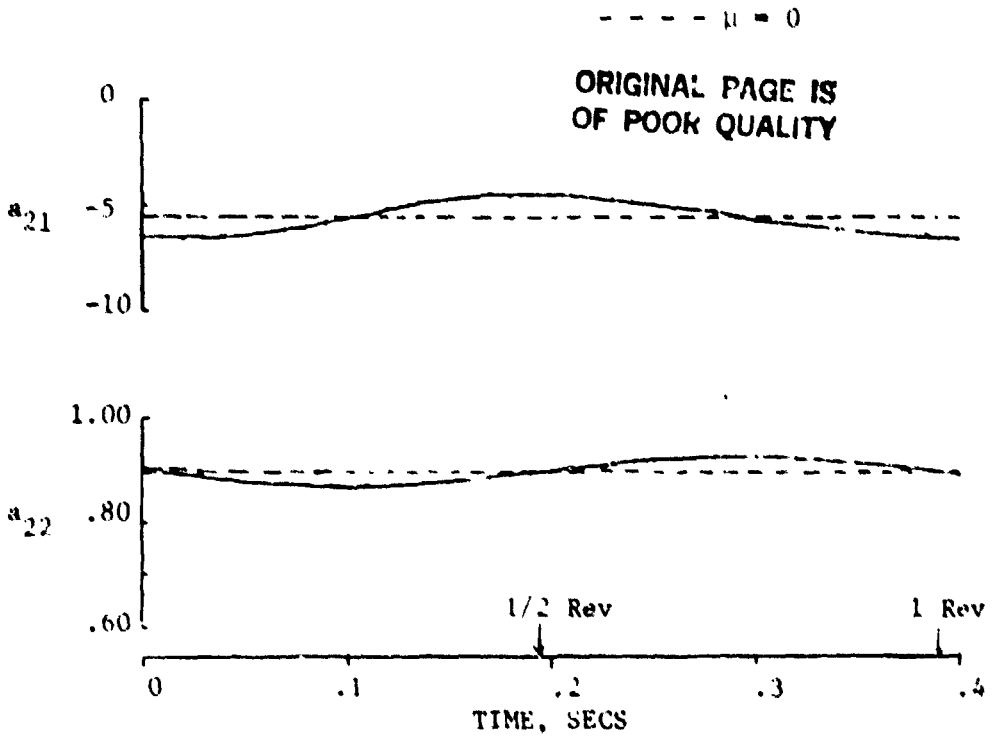

Figure 5. - Rotor Flap Model Periodic Coefficient Variation of A-Matrix (μ = .2, Small Periodicity, Negligible Reverse Flow).

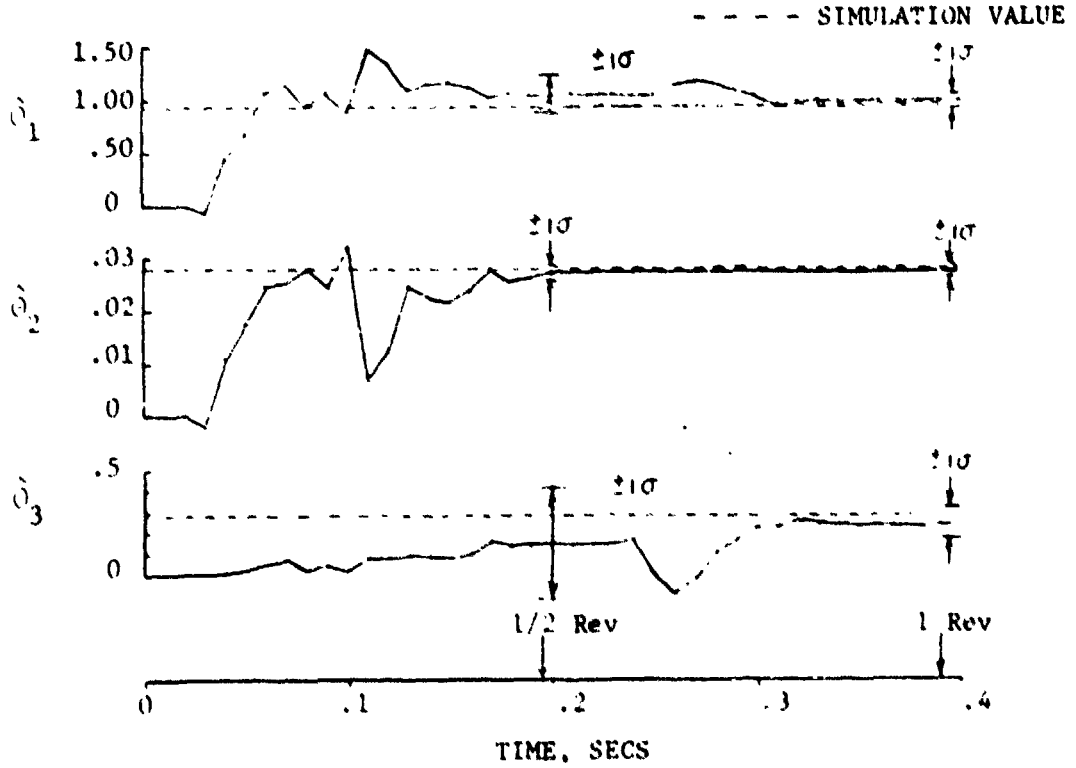

Figure 6. - Rotor Flap Model Identified Parameter Convergence, μ = .2 (Reverse Flow Coeff. Not Identified).

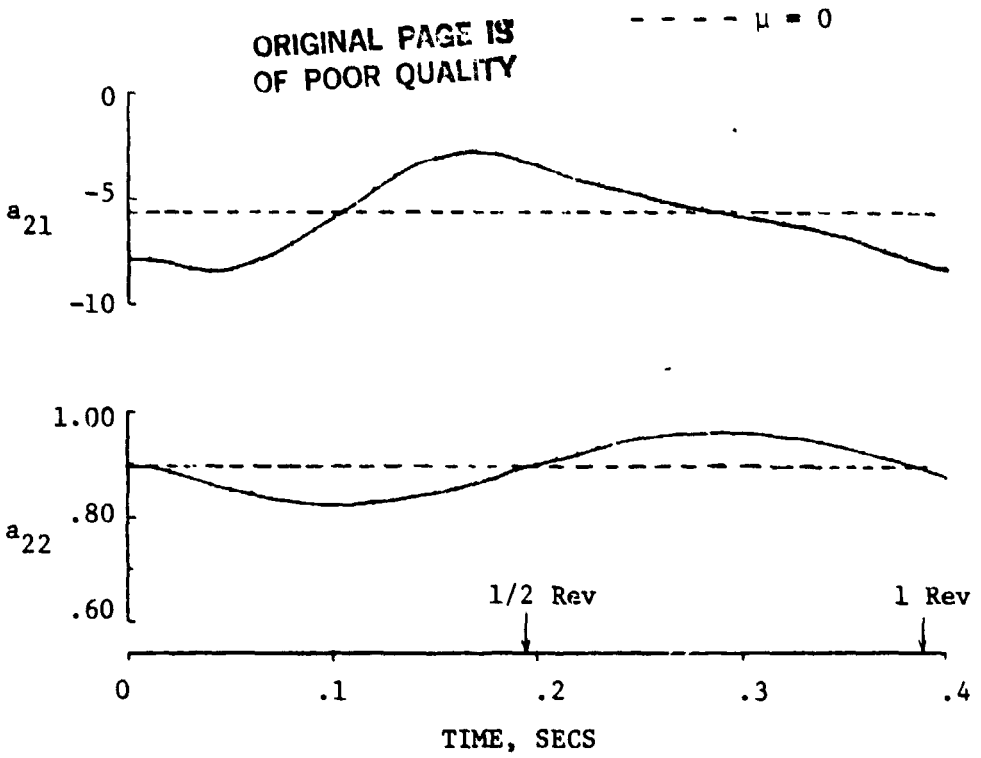

Figure 7. - Rotor Flap Model Periodic Coefficient Variation of A-Matrix (μ = .5, Moderate Periodicity, Small Reverse Flow).

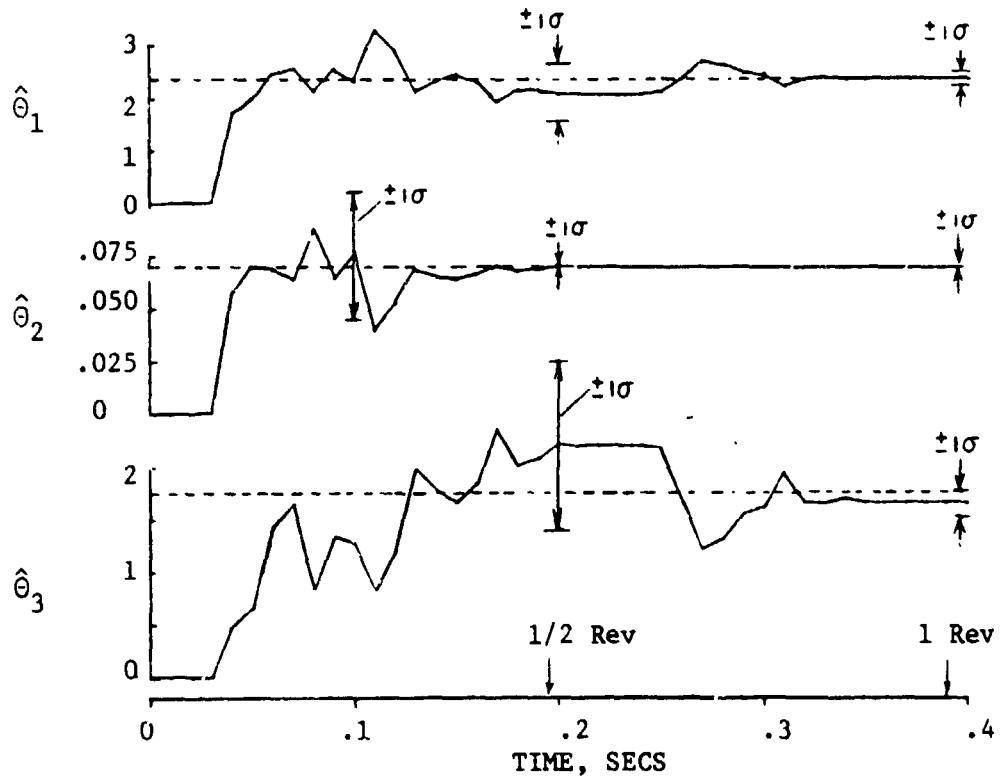

Figure 8. - Rotor Flap Model Identified Parameter Convergence, μ = .5 (Reverse Flow Coeff. Not Identified).

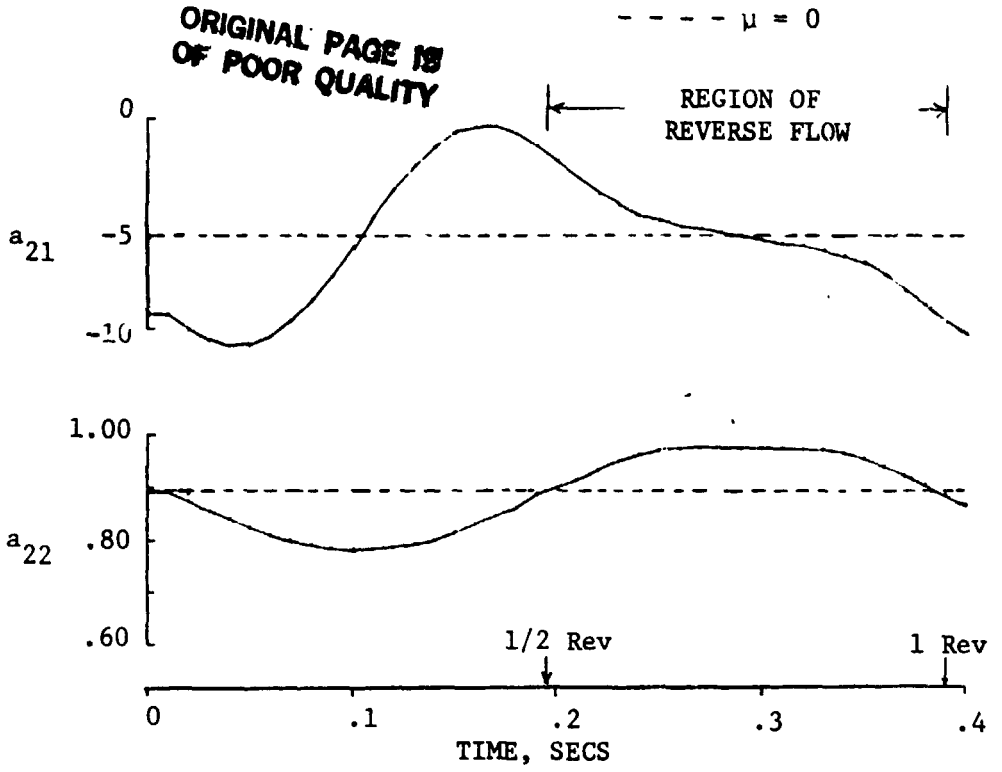

Figure 9. - Rotor Flap Model Periodic Coefficient Variation of A-Matrix (μ = .8, Strong Periodicity, Reverse Flow).

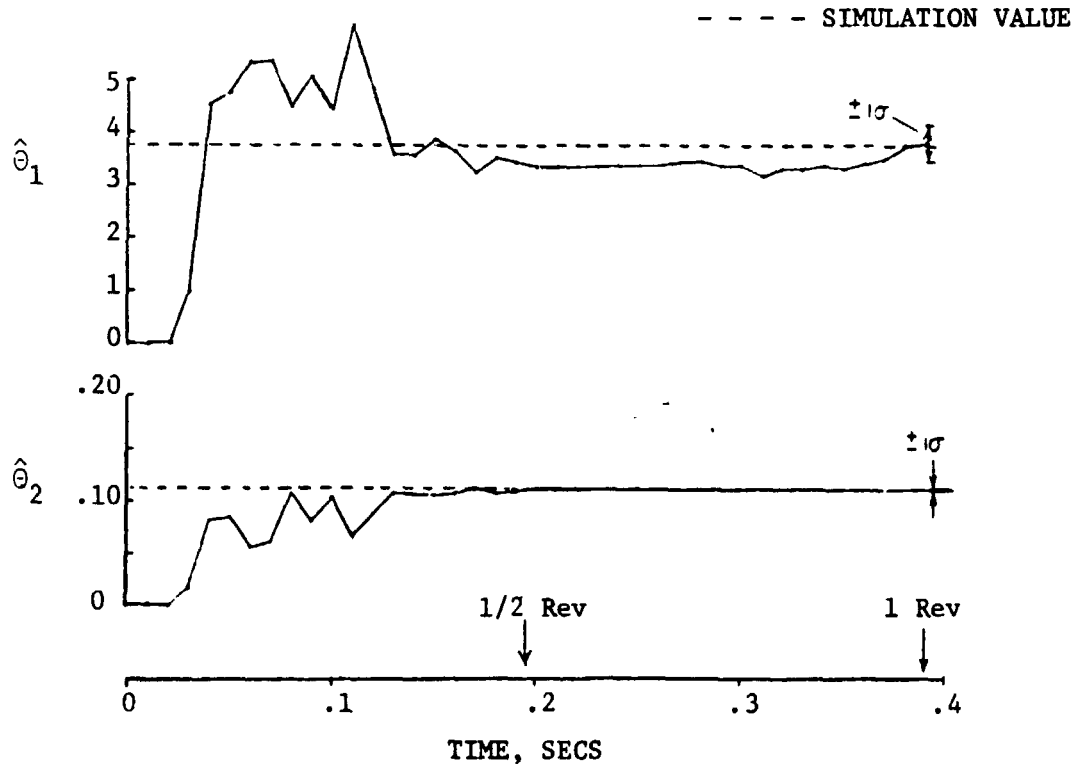

Figure 10. - Rotor Flap Model Identified Parameter Convergence, μ = .8 (cos ψ, sin ψ Coefficients, 1st Revolution).

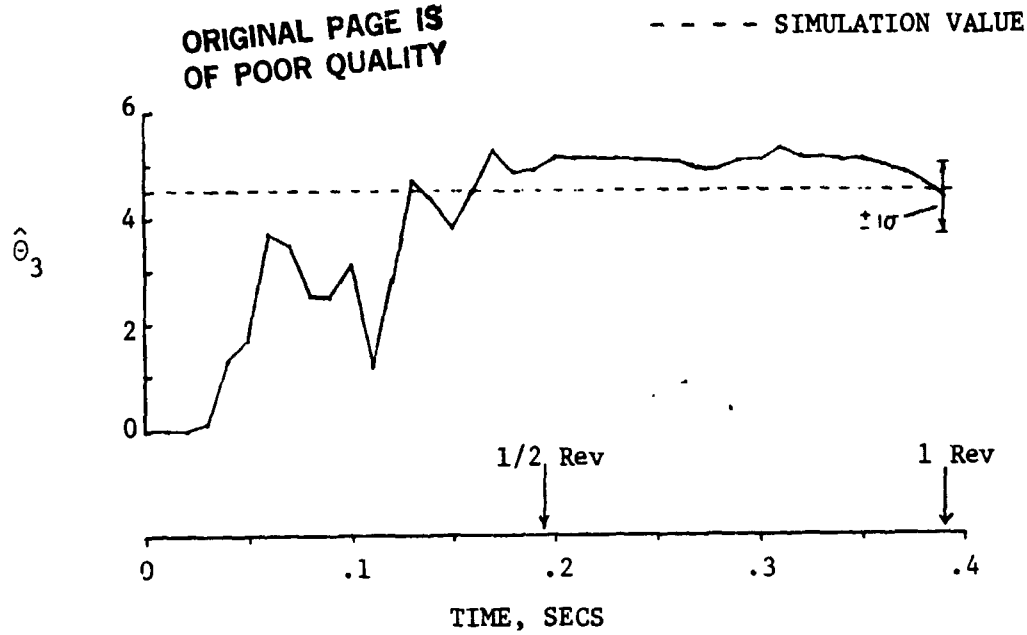

Figure 11. - Rotor Flap Model Identified Parameter Convergence, μ = .8 (cos ψ sin ψ Coefficient)

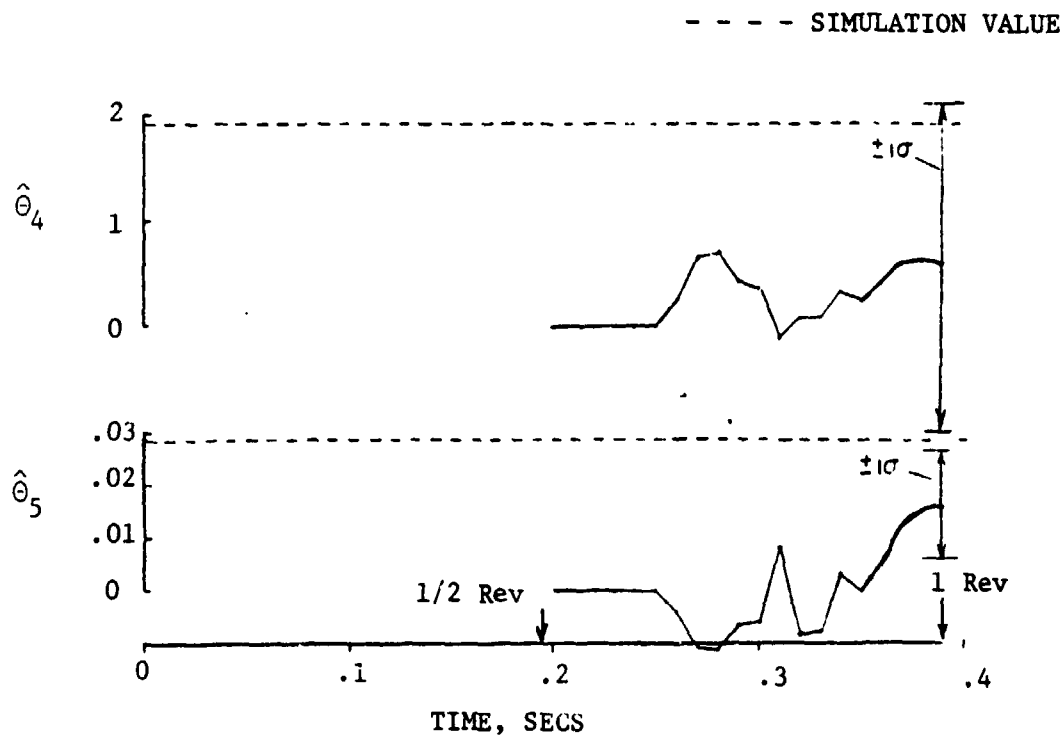

Figure 12. - Rotor Flap Model Identified Parameter Convergence, μ = .8 (Reverse Flow Coefficients).

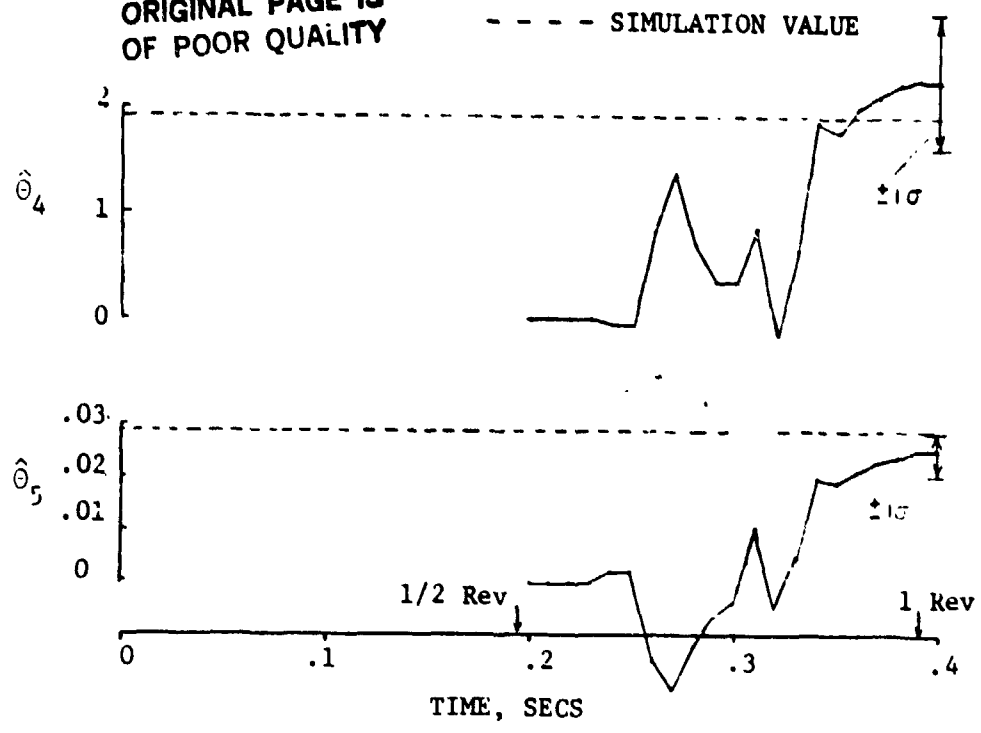

Figure 13. - Rotor Flap Model Identified Parameter Convergence, μ = .8 (Reverse Flow Coeff., Signal x 3).

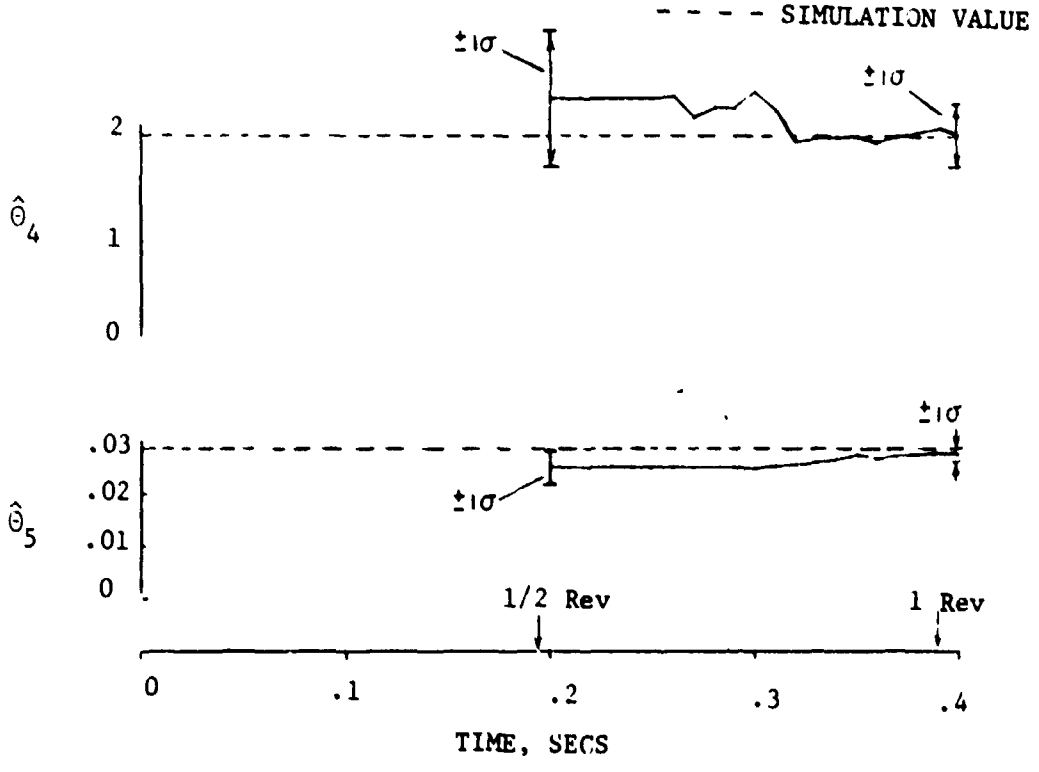

Figure 14. - Rotor Flap Model Identified Parameter Convergence, μ = .8 (Reverse Flow Coeff., Signal x 3).

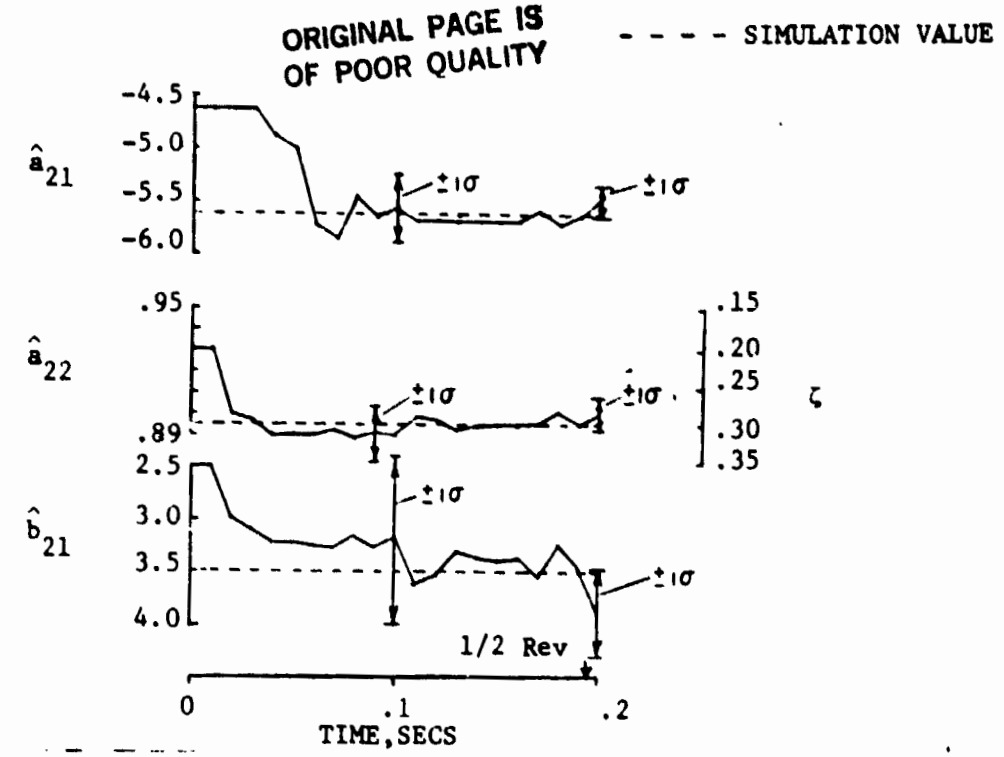

Figure 15. - Rotor Flap Model Identified Parameter Convergence for the CE Stochastic Controller, μ = 0.

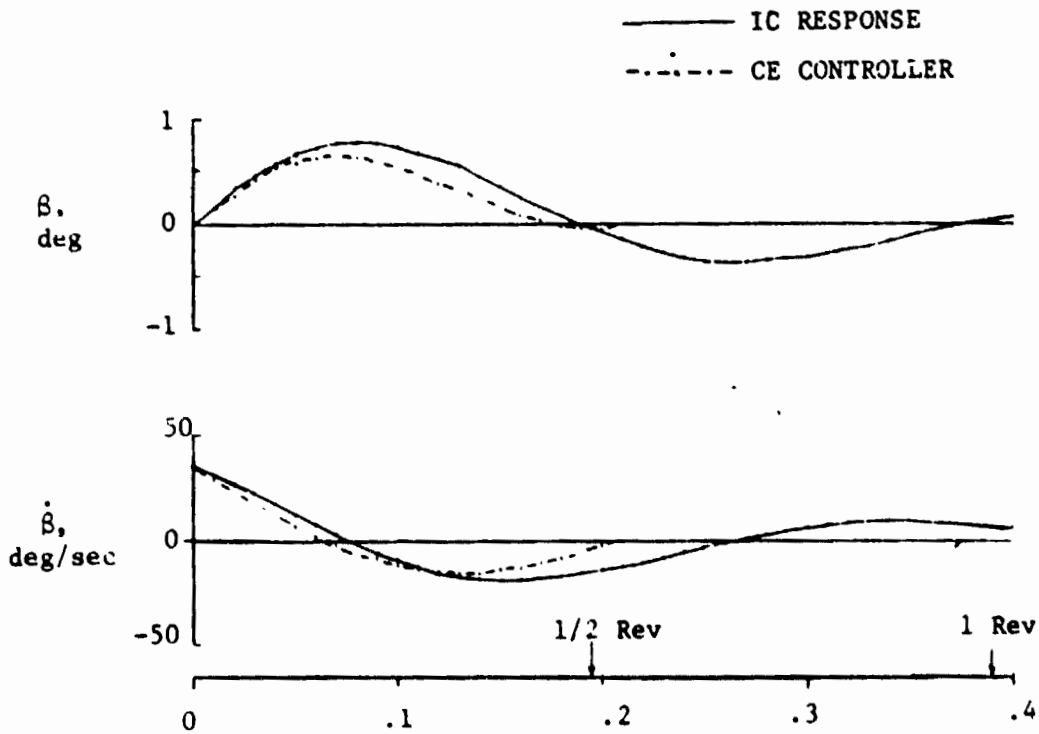

Figure 16. - Rotor Flap Model State Time History Response Comparing Open Loop Free Response with CE Controlled Response.

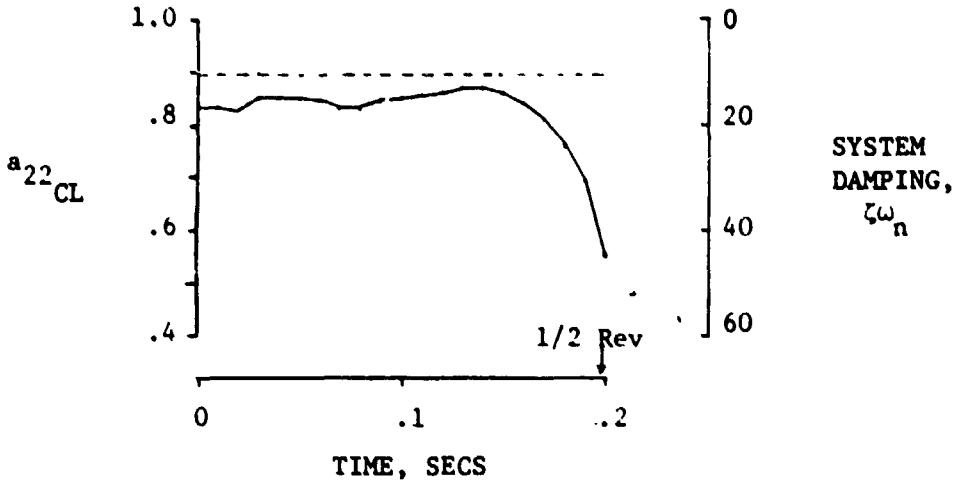

Figure 17. - Rotor Flap Model Equivalent Closed Loop System Damping, CE Control, $\mu = 0$ (Time Varying, $A_{CL} = A-B\hat{k}$).

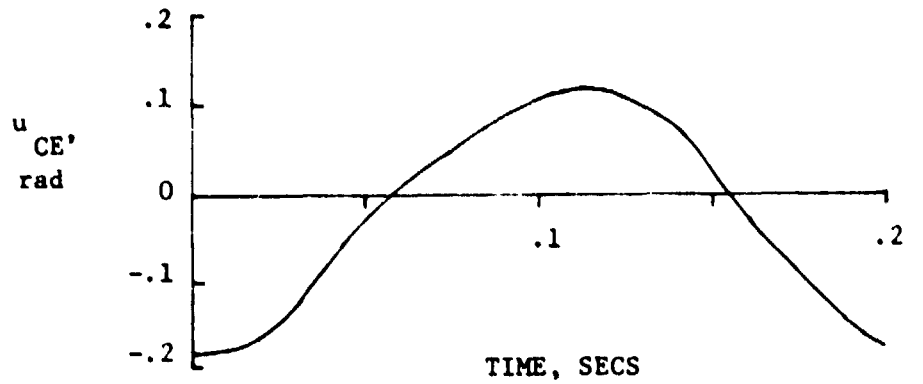

Figure 18. - Rotor Flap Model Feedback Control Time History Response, CE Control, $\mu = 0$.

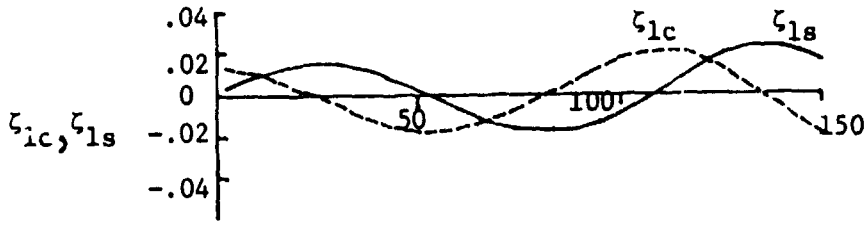

Figure 19. - Ground Resonance Rotor Model State Response, IC Set 2, Ω = 150 RPM.

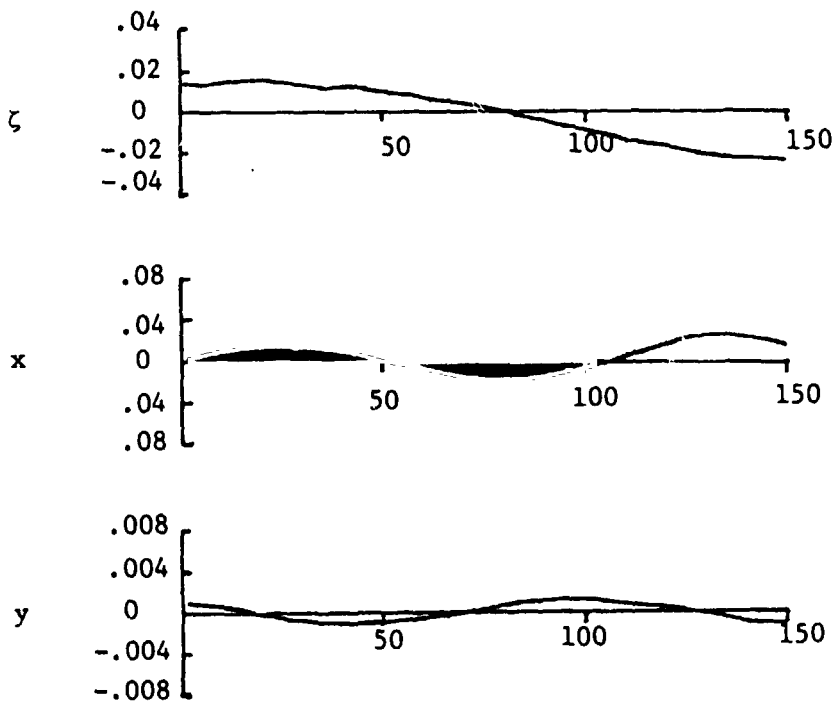

Figure 20. - Ground Resonance Model Measurement Response, IC set 2, Ω = 150 RPM (Rotating Rotor Measurement).

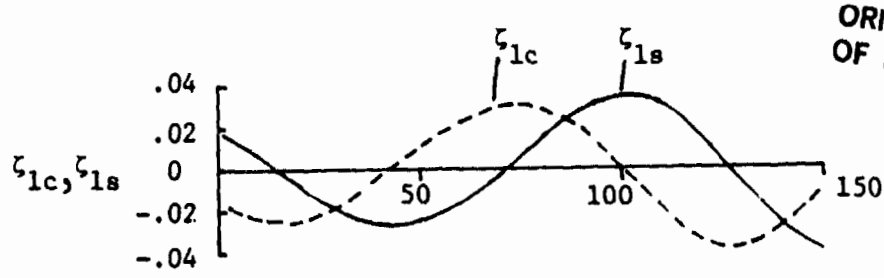

Figure 21. - Ground Resonance Rotor Model State Response, IC Set 3, Ω = 150 RPM.

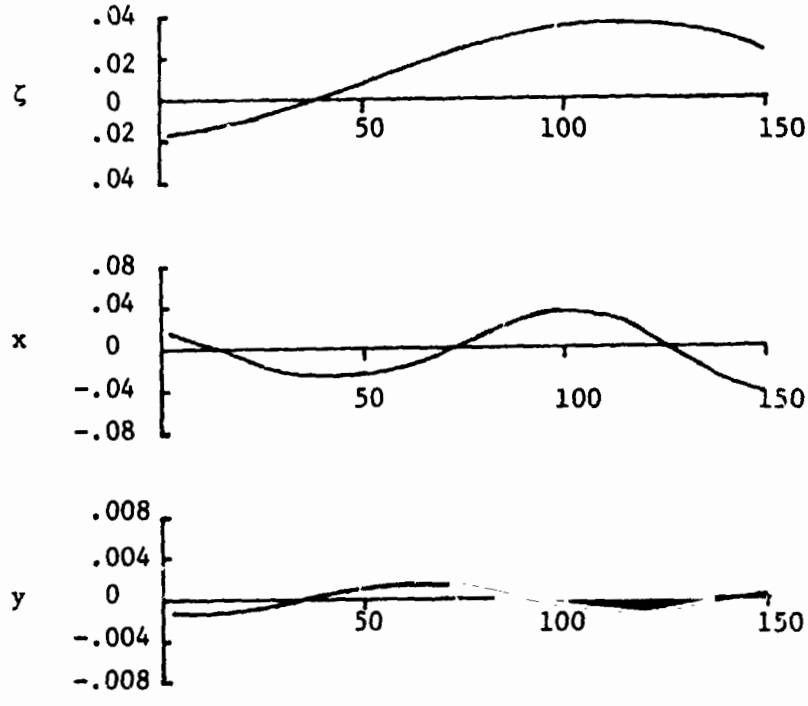

Figure 22. - Ground Resonance Model Measurement Response, IC Set 3, Ω = 150 RPM (Rotating Rotor Measurement).

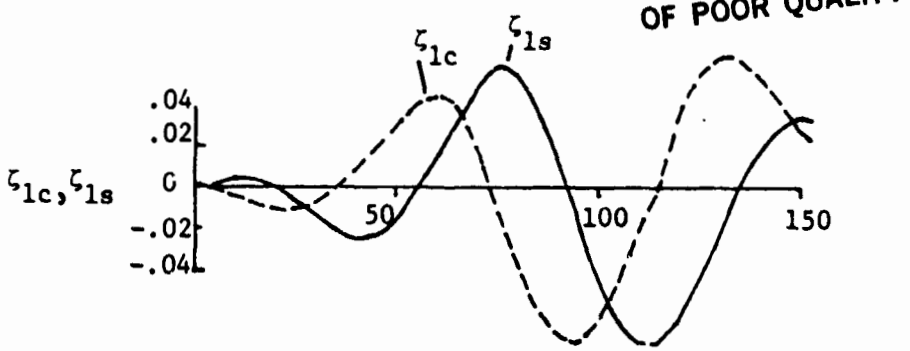

Figure 23. - Ground Resonance Rotor Model State Response, IC Set 5, Ω = 150 RPM.

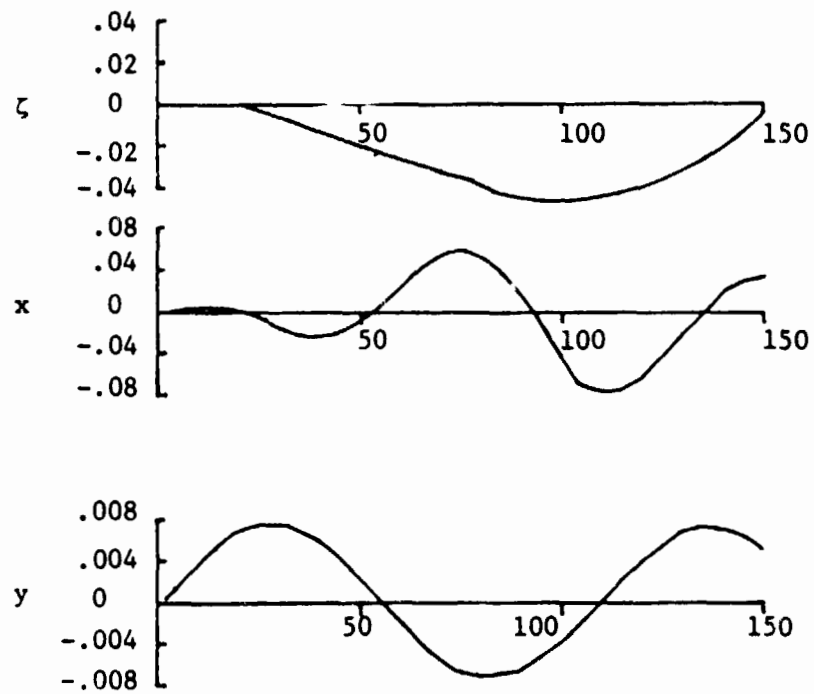

Figure 24. - Ground Resonance Model Measurement Response, IC Set 5, Ω = 150 RPM (Rotating Rotor Measurement).

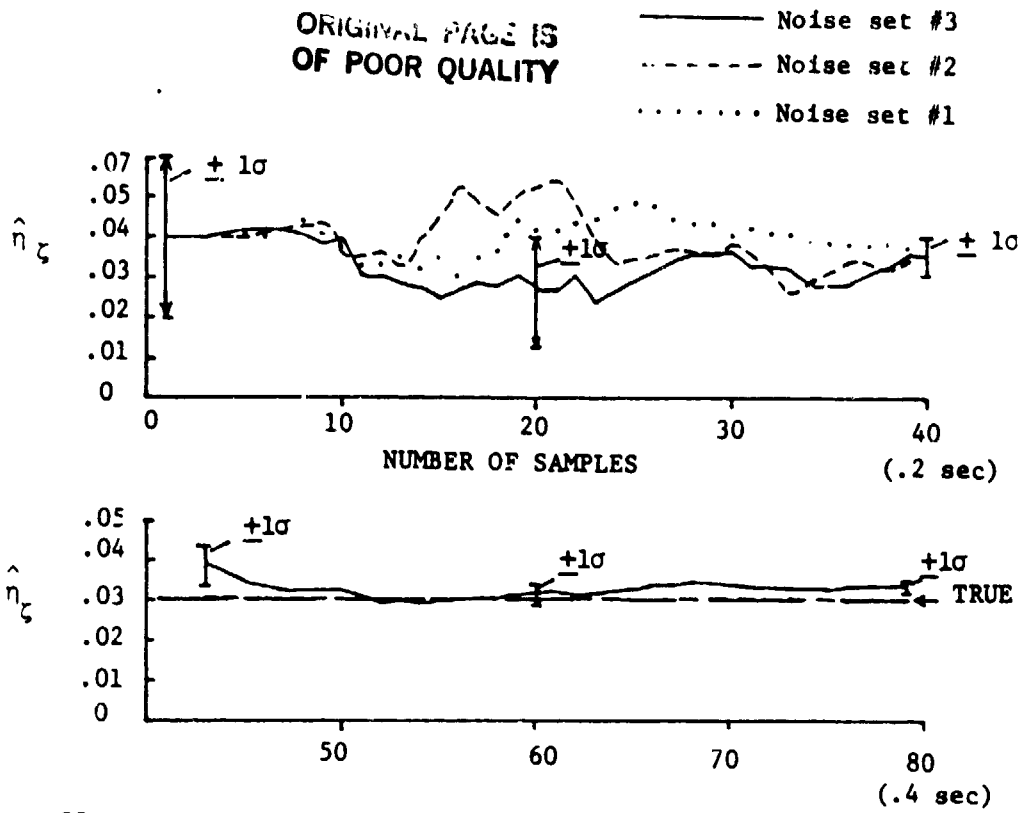

Figure 25. - Ground Resonance Model Identified Parameter Convergence Compari- Three Random Noise Sequences (Q^{Θ} = 0, IC set 1, Ω = 150 RPM)

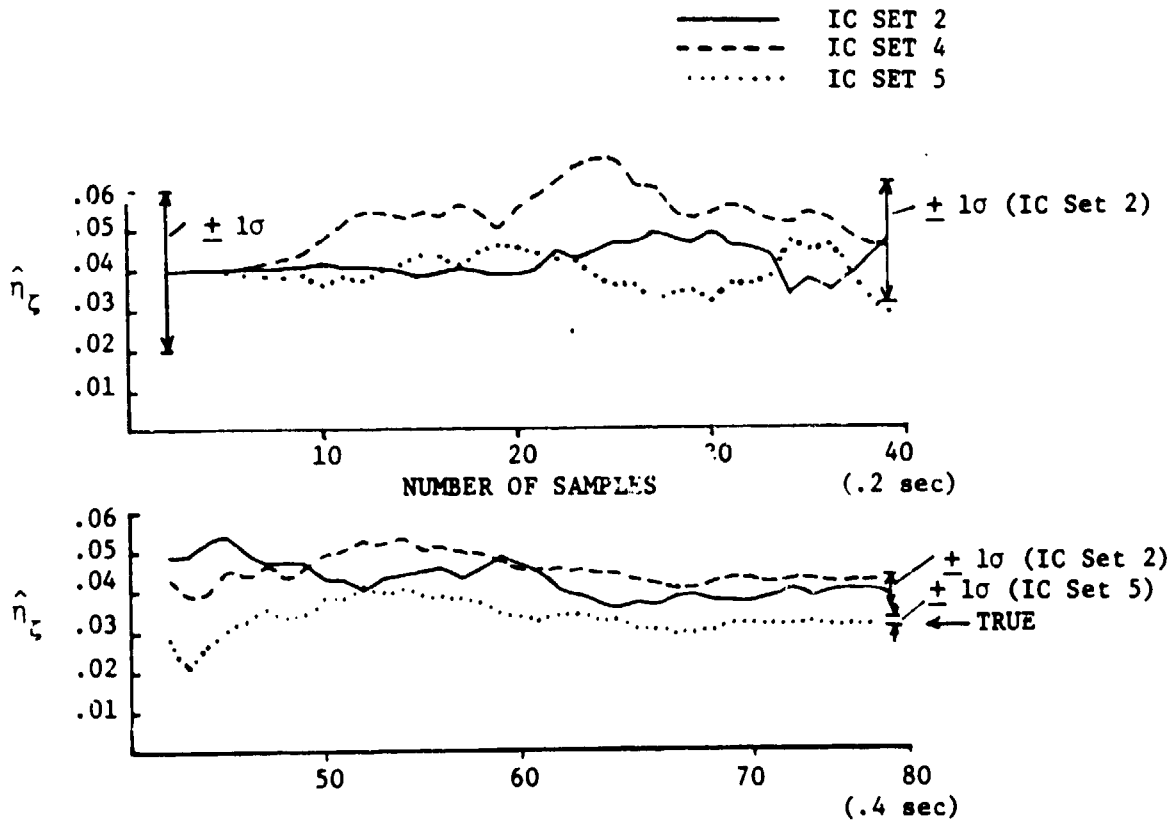

Figure 26. - Ground Resonance Model Identified Parameter Convergence Comparing Different Initial Condition Sets (Noise Set 3, Q^{Θ} = 0, Ω = 150 RPM).

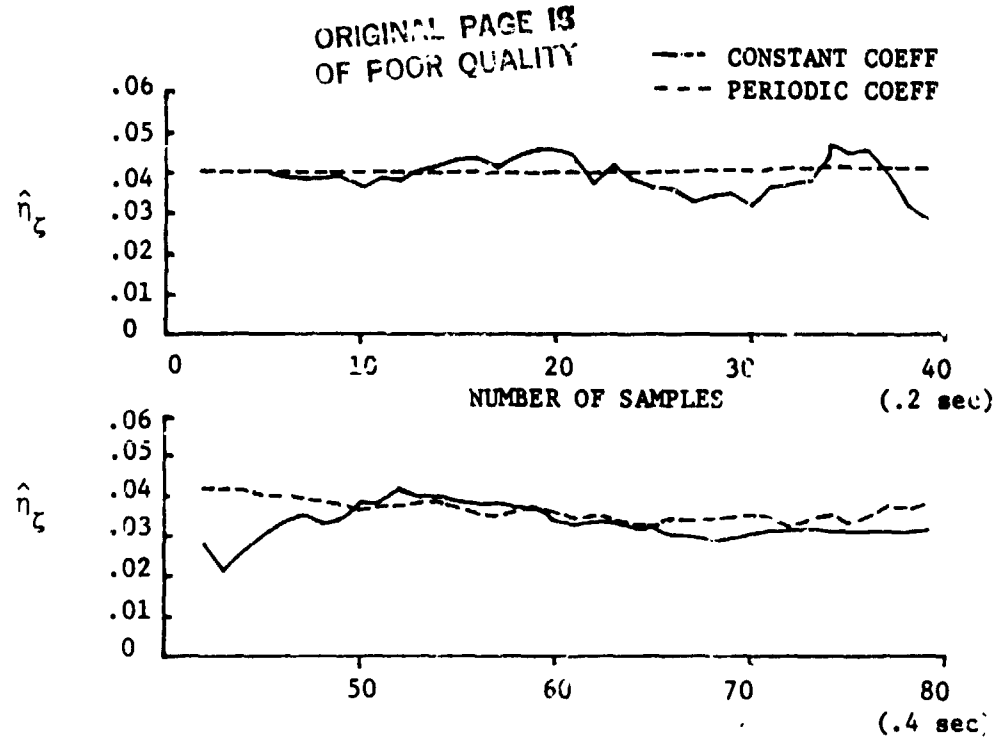

Figure 27. - Ground Resonance Model Identified Parameter Convergence Comparing Periodic and Constant Coefficient Model (IC Set 5, Q^{Θ}= 0, Ω = 15.1 RPM).

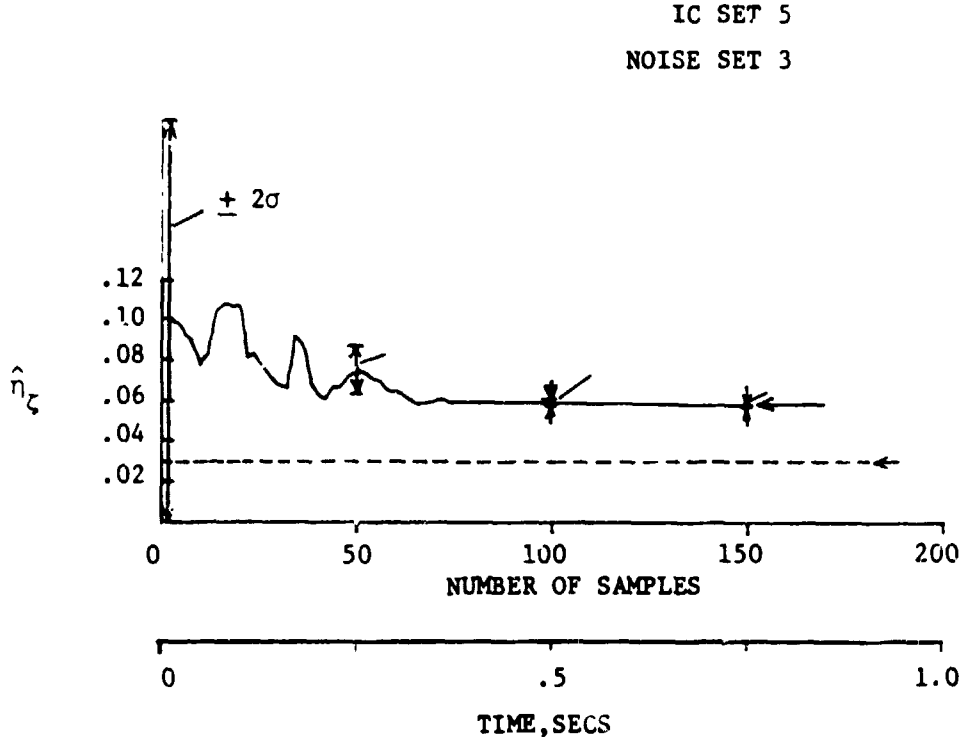

Figure 28. - Ground Resonance Model Identified Damping Parameter Convergence Using Multiblade Lag Measurement (Constant Coefficient Measurement Model, Process Noise Covariance of Parameter Q^{Θ} = 0).

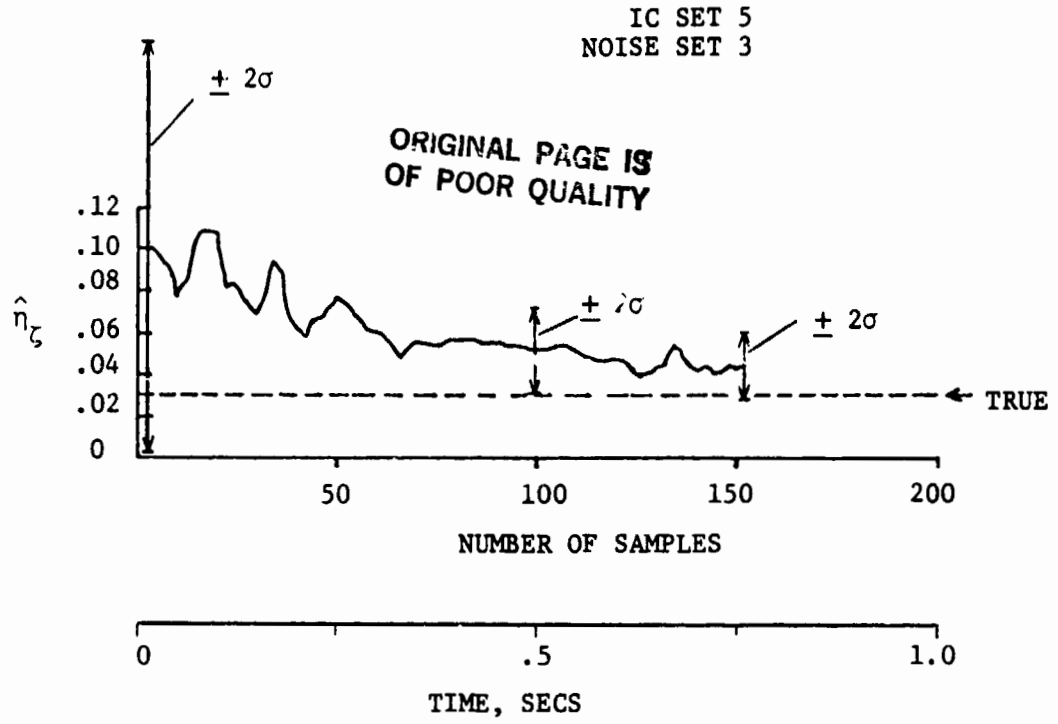

Figure 29. - Ground Resonance Model Identified Damping Parameter Convergence Using Multiblade Lag Measurement (Constant Coefficient Measurement Model) Process Noise Covariance of Parameter $Q^{\Theta} = 4x10^{-6}$).

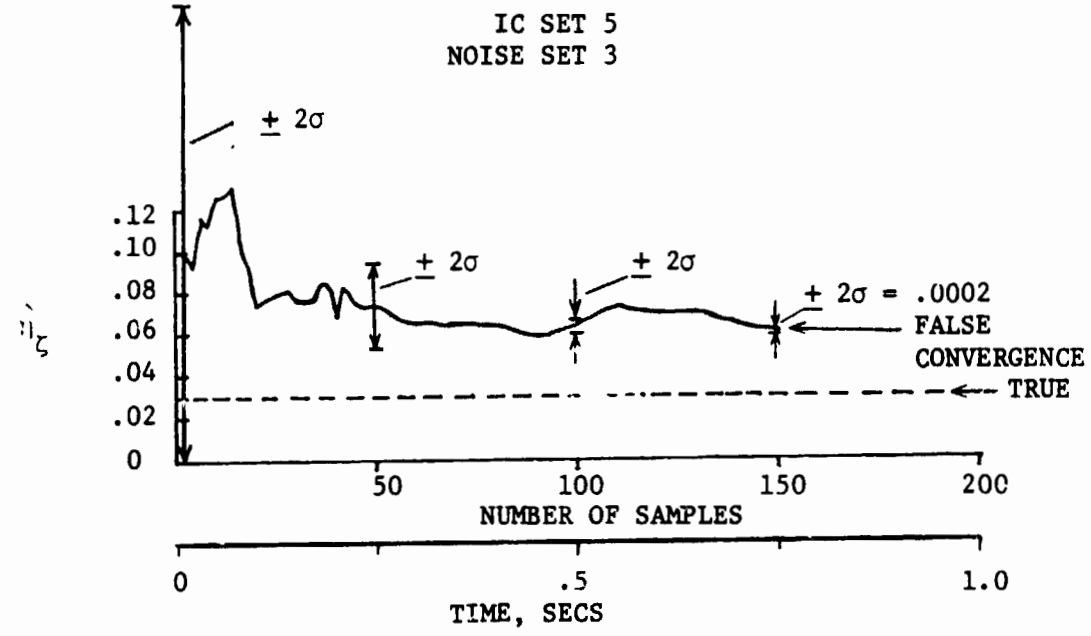

Figure 30. - Ground Resonance Model Identified Damping Parameter Convergence Using Blade Lag Measurement (Periodic Measurement Model) Showing False Convergence when $Q^{\Theta} = 0$.

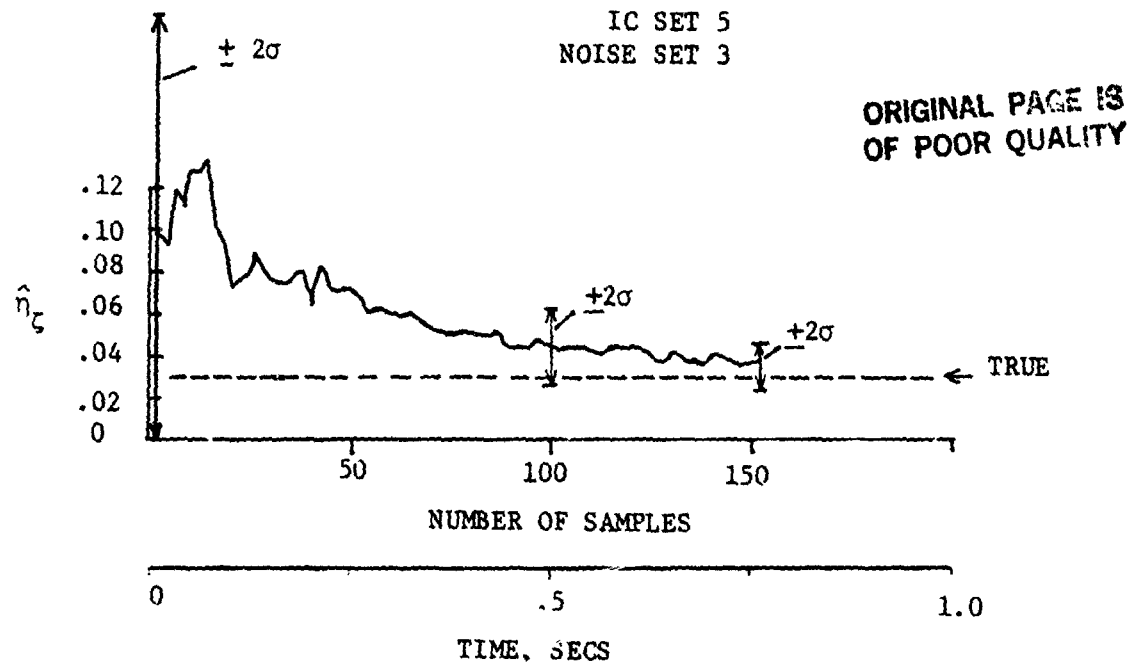

Figure 31. - Ground Resonance Model Identified Damping Parameter Convergence Using Blade Lag Measurement (Periodic Measurement Model) (Process Noise Covariance of Parameter $Q^{\Theta} = 4x10^{-6}$).

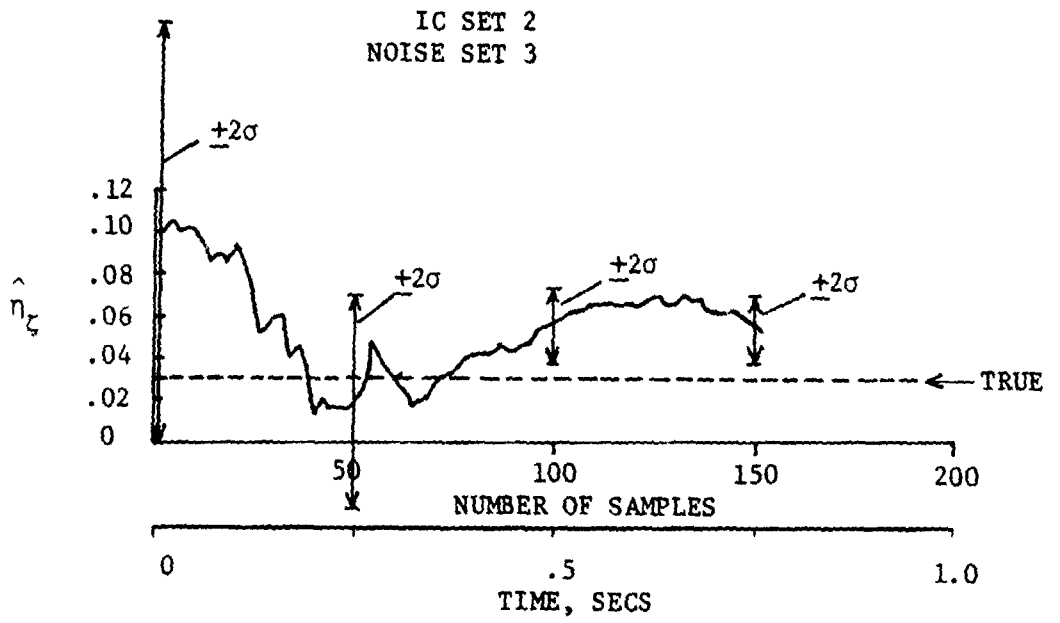

Figure 32. - Ground Resonance Model Identified Damping Parameter Convergence (Periodic Model, $Q^{\Theta} = 4x10^{-6}$, IC Set 2 from Stick Stirring, Ω = 150 RPM).

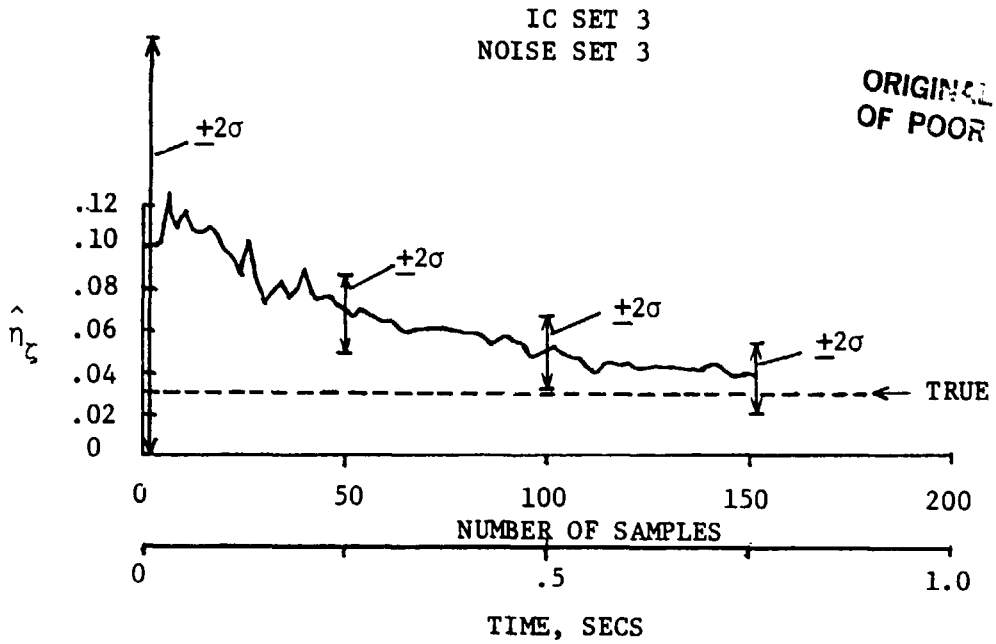

Figure 33. - Ground Resonance Model Identified Damping Parameter Convergence (Periodic Model. $Q^{\Theta} = 4 \times 10^{-6}$, IC Set 3 from Stick Stirring, Ω = 150 RPM).